

1 **Stable isotope ecology of Cape dune mole-rats (*Bathyergus suillus*) from Elandsfontein,**
2 **South Africa: implications for C₄ vegetation and hominin paleobiology in the Cape Floral**
3 **Region**

4
5 David B. Patterson^{1*}, Sophie B. Lehmann³, Thalassa Matthews⁴, Naomi E. Levin³, Deano
6 Stynder⁵, Laura C. Bishop⁶, David R. Braun^{2,4,7}

7
8
9
10
11 ¹Hominid Paleobiology Doctoral Program, Center for the Advanced Study of Human
12 Paleobiology, The George Washington University

13 ²Center for the Advanced Study of Human Paleobiology, The George Washington University

14 ³Department of Earth and Planetary Sciences, Johns Hopkins University

15 ⁴Iziko Museums of South Africa, Cape Town, South Africa

16 ⁵Department of Archaeology, University of Cape Town

17 ⁶Faculty of Science, Liverpool John Moores University

18 ⁷Department of Human Evolution, Max Planck Institute for Evolutionary Anthropology

19

20

21

22

23 * Corresponding Author

24

25 Keywords: *Bathyergus*, isotope ecology, C₄, hominin, Elandsfontein, mid-Pleistocene

26

27 **Abstract**

28 The archaeological and paleontological records from the west coast of South Africa have
29 potential to provide insights into ecosystem dynamics in the region during the mid-Pleistocene.
30 Although the fossil record suggests an ecosystem quite different than that of the region today,
31 we understand little about the ecological factors that contributed to this disparity. The site of
32 Elandsfontein (EFT) dates to between 1.0 and 0.6 million years ago (Ma), preserves *in situ* lithic
33 and faunal materials found in direct association with each other, and provides the rare
34 opportunity to examine the relationship between hominin behavioral variability and landscape
35 heterogeneity in a winter rainfall ecosystem. In this study, we examine the stable carbon
36 isotopic composition of a large sample (n = 81) of Cape dune mole-rats (*Bathyergus suillus*) and
37 contemporaneous large mammals (> 6 kg; n = 194) from EFT. We find that $\delta^{13}\text{C}$ values of *B.*
38 *suillus* are significantly different to those of contemporaneous large mammals from EFT
39 indicating a significant presence of plants utilizing the C₄ photosynthetic pathway during the
40 mid-Pleistocene, in contrast to present C₃ dominated ecosystems along the west coast of South
41 Africa. Additionally, we find that artifact density at EFT localities is positively correlated with $\delta^{13}\text{C}$
42 values in *B. suillus* enamel suggesting that evidence of more intense hominin occupation may
43 be associated with the presence of more C₄ vegetation. Lastly, we hypothesize that this unique
44 distribution of vegetation 1) provided abundant resources for both hominin and non-hominin
45 taxa and 2) may have concentrated hominin and animal behavior in certain places on the
46 ancient landscape.

47

48

49

50

51

52

53 **1. Introduction**

54 **1.1 Southern African Paleoecosystems**

55 Differing combinations of climatological factors influence ecosystem dynamics in eastern
56 and southern Africa (Levin, 2015). As a result, placing the rich Quaternary fossil records of
57 these two regions within a resolute ecological framework requires the integration of marine and
58 terrestrial proxies reflective of a variety of spatial and temporal scales (deMenocal, 2004;
59 Behrensmeyer, 2006; Behrensmeyer and Reed, 2013). The last 1 million years of the African
60 fossil record is particularly interesting because it witnesses many important shifts in mammal
61 clades (Vrba, 1995; Faith, 2011; Patterson et al., 2014), as well as the blossoming of what many
62 consider the behavioral repertoire of modern humans (McBrearty and Brooks, 2000; Marean et
63 al., 2007). Although the integration of high-resolution paleoecological data has proved
64 successful at many eastern African localities (Potts et al., 1999; Tryon et al., 2014, 2015; Faith
65 et al., 2015), much less is understood about ecosystems and faunal communities in southern
66 Africa during a critical time period in mammalian evolution. As a result, extrapolating the
67 paleoenvironmental conditions of eastern Africa to concurrent time periods in southern Africa
68 has been especially challenging (Patterson et al., 2014).

69 In southern Africa, differences in the seasonal distribution of precipitation are largely
70 responsible for the geographic distribution of vegetation (Chase and Meadows, 2007). In the
71 summer rainfall zone (SRZ), the majority of precipitation falls between October and March. In
72 contrast, the winter rainfall zone (WRZ), a narrow band incorporating the western and part of the
73 southern coasts, receives the majority of its rainfall between April and September (Fig. 1).
74 Between these two regions is the year-round rainfall zone (YRZ) that receives rainfall
75 throughout the year. Although the extent of these zones are clearly discernable in contemporary
76 southern Africa, their distribution over the past million years is far from understood. It is,
77 however, becoming increasingly clear that oscillations in atmospheric and oceanic circulation as

78 well as glacial and interglacial cycles affected the location, duration and intensity of rainfall in
79 these regions during the Quaternary (Chase and Meadows, 2007).

80 **INSERT FIGURE 1**

81 The relationship between precipitation and vegetation in southern Africa is most evident
82 in the distribution of plants utilizing the C₃ and C₄ photosynthetic pathways. Globally, C₄ plants
83 are adapted to low- to mid-elevation tropical systems with high temperatures and warm season
84 precipitation, while C₃ plants are dominant in regions of higher elevation with lower
85 temperatures and cool season precipitation (Tieszen et al., 1979; Ehleringer et al., 1997). In the
86 SRZ, C₄ plants dominate plant communities (Vogel et al., 1978; Rebelo et al., 2006; Radloff,
87 2008). In the WRZ, however, with the exception of a few common plant communities (e.g.,
88 strandveld, renosterveld) that contain species that utilize the C₄ pathway, C₃ vegetation
89 dominates in the form of the low-height, shrubby, fire-adapted fynbos (Cowling, 1992). This
90 unique vegetation system primarily within the WRZ, classified as the Cape Floral Region (CFR),
91 is host to nearly 9,000 plant species, a majority (69%) of which are endemic (Cowling, 1992;
92 Cowling and Lombard, 2002; Goldblatt and Manning, 2002; see Marean, 2010 for summary).
93 Within the CFR, differences in the proportion of C₃ and C₄ vegetation are primarily related to the
94 relative abundance of C₃ and C₄ grasses (Bar-Matthews et al., 2010). C₃ grasses are the most
95 common grasses in the WRZ, while the YRZ contains a mixture of C₃ and C₄ grasses. In the
96 SRZ, C₄ grasses are more abundant. The vegetative diversity within the CFR is not mirrored in
97 mammalian diversity (Klein, 1983). Due to the dominance of nutrient-poor fynbos vegetation, the
98 contemporary CFR does not support a sizable community of large-bodied grazing and browsing
99 ungulates, but rather is dominated by small-bodied, browsing taxa (Skead, 1980; Klein, 1983).

100 Although C₃ plants are present in high frequencies in the modern vegetative
101 communities in the CFR (Cowling, 1992), this may not always have been the case. The timing
102 and underlying climatological drivers of plant distributions in the CFR remain enigmatic. Marine
103 records from the region beginning in the Miocene indicate an overall increase in aridity with

104 multiple phases of vegetation change alongside relative stability in moisture availability (Maslin
105 et al., 2012; Hoetzel et al., 2013, 2015). More recent stable carbon isotopic analyses of
106 mammalian enamel suggest the presence of C₄ vegetation in the CFR during certain periods of
107 the Quaternary (Luyt et al., 2000; Hare and Sealy, 2013). Much like elsewhere on the African
108 continent, however, the integration of C₄ vegetation into the CFR plant biome would have likely
109 been highly heterogeneous within a C₃ dominated system (Feakins et al., 2013). This scenario
110 is supported by the lack of evidence for C₄ grasses at Langebaanweg approximately 5 Ma (Ma
111 = million years ago; Franz-Odenal et al., 2002; Rossouw et al., 2009), and evidence of their
112 presence at younger sites of Elandsfontein (Luyt et al., 2002) and Hoedjiespunt (Hare and
113 Sealy, 2013) dating to approximately 1.0 – 0.6 Ma and 0.35 – 0.25 Ma respectively. Thus,
114 although these data suggest that C₄ plants were represented in the CFR during the Quaternary,
115 we understand little about their overall spatial and temporal distribution.

116 Much of the uncertainty about the relative contribution of C₃ and C₄ vegetation in the
117 CFR during the Quaternary can be attributed to a spatially and temporally discontinuous
118 terrestrial paleoclimatic record (Carr et al., 2006). Although the region is host to a rich record of
119 mammalian fossils spanning the Miocene to Holocene (Singer and Heltne, 1966; Hendeby, 1974;
120 Volman, 1978; Klein et al., 2007; Marean et al., 2010; Braun et al., 2013a), robust connections
121 between climate and terrestrial ecosystem dynamics are limited to a few well-studied records
122 that are geographically dispersed throughout the CFR. The fossil record suggests that the CFR
123 was drastically different during the Quaternary and was populated with large grazing and
124 browsing herbivores that are absent from the region today (Klein et al., 2007; Stynder, 2008). In
125 addition, this region was host to some of the earliest populations of humans that exhibited
126 ‘modern’ behavior in terms of their manufacture of artifacts and utilization of resources
127 (Henshilwood et al., 2002; Marean et al., 2007; Brown et al., 2009). This unique and highly

128 dynamic system is unlike that of the region today and requires further investigation to provide
129 insights into the ecosystem-level drivers of this disparity.

130

131 **1.2 Study site**

132 The mid-Pleistocene eolian sediments of Elandsfontein (EFT) present a unique
133 opportunity to investigate the nature of paleoecosystems within the CFR during the past 1
134 million years (Fig. 1). These deposits (approximately 11 km²) contain an extensive record of
135 both hominin and non-hominin ecological and behavioral evolution between 1.0 and 0.6 Ma
136 (Braun et al., 2013a). With *in situ* associated fossils and artifacts, EFT presents the prospect of
137 illuminating the ecological dynamics within a WRZ paleocommunity during an enigmatic period
138 in the southern African record (Fig. 2). Although there are localities in the region of older (Franz-
139 Odendaal et al., 2002) and younger age (Berger and Parkington, 1995; Dietl et al., 2005;
140 Matthews et al., 2005; Klein et al., 2007; Faith and Behrensmeyer, 2013; Hare and Sealy,
141 2013), EFT represents a rare window into the ecosystem and faunal community of the CFR
142 during a period unrepresented at other sites (Klein et al., 2007).

143

INSERT FIGURE 2

144 Paleontological and archaeological research at EFT has occurred intermittently over the
145 past 50 years. Initial investigations into the EFT deposits resulted in the recovery of a hominin
146 calvarium referred to as the “Saldanha” or “Hopefield” specimen (Drennen, 1953), a number of
147 large cutting tools from a site called Cutting 10 as well as a tremendous quantity of non-hominin
148 mammalian fossils (Singer and Wymer, 1968; Deacon, 1998; Klein et al., 2007). Subsequent
149 collections during the 1960s and 1980s were the result of non-systematic surface surveys over
150 a relatively small portion (~3 km²) of the extent of the dunefield at EFT (Avery, 1989; Klein et al.,
151 2007). More recently, analyses were focused on collections of contextually uncertain fossil
152 material from deflation surfaces across the dunefield; this collection is referred to as
153 “Elandsfontein Main” and consists of well over 20,000 identified specimens (Klein, 1988; Klein et

154 al., 2007). The collection consists of an extremely diverse mammalian fauna dominated by large
155 browsing and grazing ungulates suggestive of a paleocommunity that was drastically different in
156 both diversity and abundance from that present in the CFR today. In addition, an analysis of the
157 stable carbon isotopic signature of mammalian enamel from the Elandsfontein Main collection
158 suggests the presence of a small amount of C₄ vegetation in the diet of ungulates from the site
159 (Luyt et al., 2000; Lehmann et al., *in Review*). Analyses of the mesowear patterns on these
160 teeth indicate that many large mammals had unexpected dietary adaptations to herbivory based
161 on their taxonomy (Stynder, 2009). Although these investigations suggest a vegetation
162 community different than that of contemporary EFT, due to the lack of precise context,
163 questions regarding the spatial and temporal nature of these patterns remain unresolved.

164 Most recently, beginning in 2008, systematic excavations and collections were
165 undertaken at EFT to provide a contextual link between environmental and hominin behavioral
166 data (Braun et al., 2013a; 2013b). These recent efforts have produced a high-resolution
167 stratigraphic framework for fossils and artifacts across the EFT dunefield and indicate that 1)
168 there are *in situ* assemblages of mammalian fossils and behaviorally associated artifacts, 2) the
169 majority of these *in situ* deposits are associated with a nodular layer in pedogenically modified
170 sands, 3) there is an older, calcretized sand horizon which also contains mammalian fossils but
171 these fossils are not abundant and are not associated with any artifacts, 4) distinguishing
172 between *in situ* materials and deposits that reflect ancient episodes of deflation is
173 straightforward using systematic excavation procedures and geologic observations (Rick, 2002),
174 and 5) hominin toolmakers transported stone to EFT for the production and use of stone tools
175 (Braun et al., 2013a).

176 The recent collections at EFT (2008-2015) have resulted in the recovery of a large
177 sample of fossil Cape dune mole-rats (*Bathyergus suillus*), which is the focus of this study. The
178 fossil remains of this relatively large, subterranean rodent (780-955 g; Bennett et al., 2009) are
179 found in substantial frequencies in many excavations in the Pleistocene sediments at EFT and

180 provide the opportunity to characterize localized vegetative environment at EFT due to the
181 restricted home range of *B. suillus*. Unlike most large mammalian ungulates that range over
182 vast territories in search of seasonally available resources, small mammals live (and die) within
183 a highly restricted space (Andrews, 1990; Reed, 1997). Before employing rodents and other
184 small mammals as indicators of paleoenvironments, however, it is crucial to determine the
185 agent/s of accumulation within a fossil assemblage (Andrews, 1990). Although small mammals
186 may die and be preserved within or close to their home range in life, their remains may be
187 transported away from their original environmental context by mammalian and avian predators
188 (Matthews et al., 2006a; Reed, 2007; Terry, 2007). If the mode of accumulation can be
189 confidently established, small mammals may provide an excellent proxy for localized
190 paleoenvironments. This study uses the stable carbon isotopic composition of *in situ* Cape dune
191 mole-rat enamel to provide the first analysis of the structure of the EFT vegetative environment
192 between 0.6 and 1.0 Ma.

193

194 **1.3 Modern *Bathyergus suillus* ecology**

195 The genus *Bathyergus* consists of two extant species endemic to southern Africa:
196 *Bathyergus suillus* (the Cape dune mole-rat) and *Bathyergus janetta* (the Namaqua dune mole-
197 rat). *B. suillus* is primarily confined to the coastal soils of the Western Cape Province, with a
198 single record from Rondawel near Groenrivier in the Northern Cape Province (Bennett et al.,
199 2009). *B. janetta* occurs in the Northern Cape Province, particularly in the Namaqualand
200 Hardeveld bioregion, Namaqualand Sandveld bioregion and some parts of the Namib desert
201 (IUCN Red List; Herbst et al., 2004). To date, fossil *B. suillus* remains are only known from sites
202 from within its historic range, the majority of which are younger than 130 Ka (Klein, 1991).
203 Previous authors have attributed fossil mole-rat material from the earlier sites of Elandsfontein
204 (Klein, 1991) and Duinefontein 2 (Klein, 1976) to *B. suillus*.

205 *Bathyergus* is largely solitary (Van Daele et al., 2007) with its spatial distribution
206 influenced primarily by resource availability. *B. suillus* abundance varies in coastal fynbos and
207 grassland settings, with high densities in grassland environments (Davies and Jarvis, 1986).
208 Additionally, the species is large-bodied relative to other African mole-rats (780-955 g) (Bennett
209 et al., 2009) and dig extensive burrows, some of which can include >400 m of interconnected
210 tunnels, and typically live within a single burrow system throughout their life (Davies and Jarvis,
211 1986).

212 Much like other African mole-rats, *B. suillus* feeds upon the underground storage organs
213 (geophytes) of certain plant species (e.g., *Othonna*, *Wachendorfia*; see Yeakel et al., 2007 for
214 summary). Unlike other African mole-rats, however, which are primarily subterranean feeders,
215 more than 60% of the diet of *B. suillus* originates from aerial vegetation pulled into the burrow
216 via the roots (Bennett et al., 2009). Robb et al. (2012) used stable carbon ($\delta^{13}\text{C}$) and nitrogen
217 ($\delta^{15}\text{N}$) isotope ratios to illuminate the diet of extant mole-rats in the CFR. The authors conclude
218 that although geophytes make up a significant proportion of the species' diets, *B. suillus* had a
219 substantially more generalized diet, including C_4 grasses, than the other mole-rat taxa of
220 *Cryptomys hottentotus* and *Georchus capensis* from the CFR.

221 *Bathyergus suillus* is preyed upon by avian, mammalian and reptilian predators (Bennett
222 et al., 2009); however, the archaeological record indicates some degree of exploitation by
223 human populations in southern Africa (Henshilwood, 1997). This species is particularly
224 vulnerable to predation when above ground and may be preyed upon by both avian and
225 mammalian carnivores. When underground, *B. suillus* is frequently predated upon by mole
226 snakes (*Pseudapis cana*) and Cape cobras (*Naja nivea*) (Bennett et al., 2009).

227

228 **1.4 Study Objectives**

229 In this study, we use carbon stable isotope data from *in situ* mid-Pleistocene *B. suillus*
230 remains systematically collected at EFT between 2008 and 2014 and address the following
231 questions:

- 232 1. Do $\delta^{13}\text{C}$ values of *B. suillus* enamel at EFT reflect the same information about mid-
233 Pleistocene vegetation as the carbon isotope data from large mammals at EFT?
- 234 2. Can we use the carbon isotope data from the fossil teeth at EFT to identify spatial
235 patterns in vegetation across the EFT dunefield?
- 236 3. What are the implications of these findings for understanding hominin paleobiology in
237 the CFR between 1.0 and 0.6 Ma?

238

239 **2. Materials and Methods**

240 **2.1 Collections**

241 All *B. suillus* material was collected as part of archaeological and paleontological
242 excavations or systematic trenches (“shovel test pits” or STPs) across the EFT dunefield
243 between 2008 and 2014 (see Braun et al., 2013a). Collections were distributed spatially based
244 upon what are referred to as Collection “Bays” which refer to deflation hollows between large
245 modern dune crests (see Braun et al., 2013a; Fig. 3).

246

INSERT FIGURE 3

247 From this collection, we selected 150 *B. suillus* upper (maxillary) incisors as candidates
248 for stable isotopic and taphonomic analyses. All *B. suillus* material analyzed here originated
249 from the artifact and fossil-rich zone (see Braun et al., 2013a). Due to their unique morphology
250 (Fig. 4), maxillary incisors can be used to distinguish the isolated incisors of *B. suillus* from
251 those of other relatively large rodent taxa (e.g., *Otomys*) in the EFT collection. We therefore
252 focused on isolated upper incisors for this study. To preclude the potential of comingling of

253 modern and fossil material, this analysis does not include any specimens recovered from the
254 artifact- and fossil-rich horizons that were in the upper ~10 – 15 cm of the STPs or excavations.

255 **INSERT FIGURE 4**

256 **2.2 Taphonomic Analysis**

257 Previous researchers have considered *B. suillus* remains from EFT to be
258 contemporaneous with other fossils and artifacts from the site (Klein, 1991). However, we
259 recognize three possibilities regarding the origin of *B. suillus* fossils within the EFT Pleistocene
260 sedimentary units: 1) *B. suillus* remains were deposited and preserved in primary context with
261 the artifacts and the other associated large mammal fossils as a result of normal mortality of *B.*
262 *suillus*, 2) *B. suillus* remains were deposited by avian and mammalian predators living at EFT
263 around the time of deposition of other fossils and artifacts from the site and are thus
264 contemporaneous with them and, 3) the *B. suillus* fossils are younger than the other materials in
265 the fossil- and artifact-rich horizons at EFT, as a product of *B. suillus* burrowing into those
266 horizons subsequent to deposition. Given that these three scenarios result in two alternative
267 temporal relationships between *B. suillus* remains and the other archaeological and
268 paleontological collections at EFT, we conducted a detailed taphonomic analysis of a subset of
269 *B. suillus* incisors prior to isotopic analyses.

270 To investigate the likelihood of secondary deposition of incisors (i.e., that the fossils
271 originated from mammalian scats or avian pellets) within the EFT collection, 33 upper incisors
272 were studied for traces of digestion and rounding on the enamel surface. When animal remains
273 pass through the digestive system of a predator, digestive acids leave a distinct signature on the
274 surface of bone or enamel in the form of etching or rounding, particularly in the area of contact
275 between enamel and dentine (Andrews, 1990; Fernandez-Jalvo and Andrews, 1992). This
276 signature can be easily discerned with a dissecting microscope. For this analysis, we use a
277 systematic protocol for evaluating the degree of etching and rounding on rodent incisors

278 (Matthews 2002; 2006b; Table 1). This methodology is akin to that of Fernandez-Jalvo and
279 Andrews (1992), however categories used here were specifically developed for the incisors of
280 *Bathyergus* and other southern African rodents. Using this protocol, each incisor within our
281 subset was photographed under magnification and rated on a scale of 0 – 4 based upon the
282 degree of etching and rounding on the enamel surface. To remove the possibility of confusion
283 with other taphonomic processes, such as etching caused by acidic/alkaline soil, specimens
284 were only scored if there was unquestionable evidence of digestion (refer to Table 1). Acid and
285 alkaline soils may also cause corrosion and etching on both enamel and dentine (Andrews,
286 1990; Fernandez-Jalvo, 1995), and could possibly be confused with digestion (see Fig. 4D, 4E,
287 4F), although there are generally differences in the manner in which this occurs. To avoid any
288 such errors, analysis erred on the conservative side and only included specimens that showed
289 clear evidence of having passed through the digestive tract of an avian or mammalian predator
290 (see Fig. 4B, 4C).

291 To further investigate the stratigraphic relationship between the fossils of *B. suillus* and
292 the other materials recovered from systematic excavations at EFT, we reviewed the
293 stratigraphic frequency of *B. suillus* fossils in relation to other materials found in these
294 excavations. Previously we conducted a related analysis to document the fact that similar finds
295 (<1cm) are found in similar frequencies as larger finds (Braun et al., 2013a). This analysis was
296 based on previous work documenting these types of patterns in the Channel Islands (Rick,
297 2002). Here we test whether the frequency of *B. suillus* fossils track the frequency of other finds
298 in these excavations. We excluded samples recovered from localities where formal
299 standardized excavations were not conducted (i.e., material was recovered from shovel test
300 pits). If the abundance of *B. suillus* fossils through the stratigraphic section closely tracks the
301 frequency of other fossils in the excavations at EFT, it would suggest that the deposition of the
302 *B. suillus* fossils and the other materials were the result of similar processes. If the frequency of
303 these two types of material deviate through the stratigraphic section, however, then there is the

304 possibility that the *B. suillus* fossils were deposited through either 1) a natural mortality event
305 occurring after mole-rats burrowed down into Pleistocene deposits or 2) deflation of younger
306 sediments that were previously stratigraphically above the Pleistocene sediments.

307

308 **2.3 Stable Isotopic Analysis**

309 **2.3.1 Analytical Methods**

310 A subset of 19 *B. suillus* incisors from EFT was analyzed for carbon and oxygen stable
311 isotope ratios using a laser ablation gas chromatograph system, coupled to a Thermo MAT 253
312 isotope ratio mass spectrometer in the Department of Earth and Planetary Sciences at Johns
313 Hopkins University. Although typically less precise than conventional, phosphoric acid digestion
314 methods (Passey and Cerling, 2006), laser ablation approaches were first used on the EFT *B.*
315 *suillus* material because they are less destructive and require less sample material than
316 conventional methods. Because the laser ablation technique samples all material in the laser
317 ablation pit, and does not select for the carbonate component, it is common to attempt removal
318 of surface organics prior to analysis (Passey and Cerling, 2006). Here, we used three different
319 approaches to evaluate the influence of contaminants on the surface of teeth: 1) gentle abrasion
320 of the surface enamel with a high speed rotary drill to remove secondary material, 2) soaking
321 the incisors for 15 minutes in 3% hydrogen peroxide (H₂O₂) to remove organic material and 3) a
322 control group in which nothing was done to the enamel surface. We analyzed a subset of teeth
323 targeted for carbon and oxygen isotopes of tooth enamel using the phosphoric acid digestion
324 method (see methods below) such that we could develop an understanding of the offset in the
325 results between these two methods that is specific to these samples, as is necessary for laser
326 ablation studies of fossil teeth.

327 In addition to the dataset of incisors analyzed for comparison to the data obtained from
328 laser ablation technique (n = 19), a large dataset of *B. suillus* upper incisors were analyzed
329 using phosphoric acid digestion method (n = 62). As with the laser ablation technique, only

330 upper incisors were analyzed. All incisors were photographed prior to sampling with a high-
331 speed rotary drill fitted with a diamond bit. Enamel powder was treated for 15 minutes with 3%
332 H₂O₂ to remove organic material and rinsed 3 times with distilled water prior to a 15 minute
333 treatment with 0.1M buffered acetic acid to remove secondary carbonate. Following this
334 treatment, samples were rinsed 3 times with distilled water and dried overnight at 60°C.
335 Samples were then loaded into silver capsules and digested in a 100% phosphoric acid bath at
336 90°C for 10 minutes. Samples were cryogenically cleaned using a custom-built automated
337 system (Passey et al., 2010) and the resulting CO₂ was analyzed for δ¹³C and δ¹⁸O on a
338 Thermo MAT 253 mass spectrometer. An acid fractionation factor of 1.00725 (90°C) was used
339 for tooth enamel following Passey et al., (2007).

340 Stable isotope ratios for all phosphoric acid digestion and laser ablation samples are
341 reported as δ values relative to Vienna Pee Dee Belemnite (VPDB) using standard per mil (‰)
342 notation, where $\delta^{13}\text{C} = (R_{\text{sample}}/R_{\text{standard}} - 1) \times 1000$, and R_{sample} and R_{standard} are the ratios of
343 heavy to light isotopes (e.g., ¹³C/¹²C, ¹⁸O/¹⁶O) of the sample and the standard, respectively.
344 During both types of stable isotope analyses, internal working enamel standards were analyzed,
345 normalized to the carbonate standard NBS-19, routinely to monitor instrument performance. For
346 the phosphoric acid method, Carrara marble, normalized to NBS-19, was also routinely
347 measured as an internal working standard. δ¹³C standard deviation of internal standards was
348 0.3‰, while that of δ¹⁸O was 0.2‰.

349 Lastly, we compare δ¹³C enamel values obtained from acid-etched, non-acid etched,
350 laser ablated and phosphoric acid digestion. Although we include the oxygen isotope results for
351 completeness in the tables of this paper, we do not discuss them in depth and instead focus on
352 the carbon isotope data.

353

354 **2.3.3 Dietary Reconstructions**

355 We use an isotopic dietary mixing model to estimate the potential contribution of C₃, C₄
356 and Crassulacean acid metabolism (CAM) vegetation to the diet of *B. suillus* at EFT. We use
357 the following equation:

358

$$359 \quad \delta^{13}C_{B.suillus} = (fC_3 * \delta^{13}C_{C_3(veg)}) + (fC_4 * \delta^{13}C_{C_4(veg)}) + (fCAM * \delta^{13}C_{CAM(veg)})$$

360

361 where *f* indicates the fraction of the different dietary inputs from plants that use the three
362 photosynthetic pathways and δ¹³C indicate published average δ¹³C values for each (Radloff,
363 2008; Kohn, 2010; Boom et al., 2014).

364 To reconstruct the ingested vegetation, we use a diet-tissue fractionation factor (ε*_{enamel-}
365 diet) of 11.1‰, which has been shown to be appropriate for small mammals (Podlesak et al.,
366 2008). The incorporation of CAM vegetation into this analysis is especially important given: 1)
367 the broad and often poorly understood isotopic signature of CAM vegetation in southern Africa
368 (Boom et al., 2014), and 2) their well-documented abundance in the CFR (Peters and Vogel,
369 2005). To incorporate CAM vegetation into our model, we use carbon isotopic values derived
370 directly from CAM vegetation in the CFR. Boom et al. (2014) characterized the isotopic
371 signature of 36 taxa of CAM plants from within the CFR. We use the average δ¹³C value for all
372 CAM plants from the CFR (-19.7 ± 4.0‰; Boom et al., 2014) because we do not know the
373 specific CAM plants that were prevalent in the region around EFT during the mid-Pleistocene.
374 For C₃ vegetation we used a δ¹³C value of -27.1 ± 1.6‰ obtained from the large (n = 480),
375 global compilation of C₃ plants by Kohn et al. (2010). For C₄ vegetation we used a δ¹³C value of
376 -12.8 ± 1.3‰ obtained by Radloff et al. (2008) for C₄ grasses in the CFR.

377 We estimate the percentage of C₄ vegetation consumed by large mammals at EFT
378 following a two-member version of the above mixing model, assuming that only C₃ and C₄
379 plants contributed to large mammal diets, where *f*_{CAM} = 0. For these estimates we use a ε*_{enamel-}

380 diet of 14.1‰ following Cerling and Harris (1999) and compare these values to those obtained
381 from the *B. suillus* model ($\epsilon^*_{\text{enamel-diet}} = 11.1\text{‰}$; Podelsak et al., 2008) that also considers the
382 influence of CAM vegetation.

383

384 **3. Results**

385 **3.1 Taphonomic Analysis**

386 In the taphonomic sample (n = 33), 18% of EFT *B. suillus* incisors in our taphonomic
387 subsample (n = 33) showed extreme signs of enamel and dentine etching as a result of
388 predation (Fig. 4; Table S1). Of the etched specimens, 5 scored greater than 1, with scores of 3
389 being the most prevalent. Many specimens, especially within the unetched category showed
390 clear signs of root marks (etching) as well as small, circular areas where both enamel and
391 dentine were dissolved (see Fig. 4). The latter could be related to intestinal etching, soil
392 microbes, or soil acidity, but additional actualistic studies are needed to confirm this possibility.

393 Our analysis of the frequency of specimens through the stratigraphic sequence suggests
394 that the fossils remains of *B. suillus* and those of other fossils from EFT are the result of similar
395 depositional processes. A clear indication of differences in depositional context is when smaller
396 specimens increase in frequency while larger specimens decrease (Rick, 2002). The upper 40
397 cm of the excavation at the 0313 locality shows this pattern suggesting the upper part of this
398 excavation is representative of a variety of depositional processes. In all other localities in this
399 analysis, however, the abundance of *B. suillus* fossils tracks that of large mammals at the EFT
400 Collection Bays (Fig. 5). Braun et al., (2013a) used the relationship between large and small
401 mammal remains within EFT excavated localities to suggest that there is little evidence of
402 deflation at certain localities. There have been previous suggestions that the fossiliferous
403 sediments at EFT represent multiple episodes of deflation and reburial in the past (Klein et al.,
404 2007). The fact that the frequency of *B. suillus* fossils follows the patterns exhibited by the larger
405 fossils suggest that 1) these assemblages do not represent ancient deflated surfaces and 2)

406 that the depositional processes that are responsible for the burial and preservation of the large
407 mammal fossils is also responsible for the presence of the *B. suillus* fossils. If the *B. suillus*
408 fossils represented instances where younger (or modern) mole-rats burrowed down into the
409 older Pleistocene sediments and died there, it is highly unlikely that they would preferentially be
410 buried in the same horizons that also had the highest frequencies of fossils.

411 INSERT FIGURE 5

412 3.2.1 Laser Ablation vs. Acid Digestion

413 Nearly all enamel surfaces sampled by laser ablation charred significantly, which
414 suggests a high proportion of impurities on the enamel surface as well as within the enamel
415 matrix. $\delta^{13}\text{C}$ values obtained by laser ablation and phosphoric acid digestion of EFT *B. suillus*
416 enamel ($n = 19$) are compared in Table 2. Average isotopic enrichment ($^{13}\text{C}\epsilon^*_{\text{laser-acid}}$) was $-5.9 \pm$
417 2.2‰ and ranged from -9.5‰ to -2.4‰ . Acceptable values, as detailed in Passey and Cerling
418 (2006) are: $^{13}\text{C}\epsilon^*_{\text{laser-acid}} = -0.5 \pm 0.8\text{‰}$. The majority of the $\delta^{13}\text{C}$ values for EFT *B. suillus* incisors
419 fall outside of the acceptable values obtained by Passey and Cerling (2006). This was true even
420 for samples treated prior to sampling with either diluted H_2O_2 or abrasion of the enamel surface.
421 As a result, we do not use any of the laser ablation data in any of the following analyses. Due to
422 the specific preservation circumstances of the *B. suillus* fossils at EFT, laser ablation is an
423 inappropriate technique for isotopic analysis. The standard deviation of $\delta^{13}\text{C}$ of JHU internal
424 tooth enamel standards analyzed in the same laser ablation sessions as the EFT *B. suillus* teeth
425 was 0.9‰ for $\delta^{13}\text{C}$ and 0.5‰ for $\delta^{18}\text{O}$, which suggests that the poor performance of EFT *B.*
426 *suillus* incisors is related to the characteristics of the EFT *B. suillus* teeth themselves and not
427 related to the performance of the laser ablation system. Enamel standards analyzed on the
428 system had an average $^{13}\text{C}\epsilon^*_{\text{laser-acid}}$ of $-1.2 \pm 0.3\text{‰}$. The poor performance on the laser system
429 may be due to the nature of preservation of fossil teeth at EFT. Previous analyses have noted
430 the low carbonate content of EFT fossil teeth (Luyt et al., 2000; Lehmann et al., *In Review*). This
431 serves as an instructive example that not all samples are appropriate for analysis by laser

432 ablation approaches. All subsequent analyses will be based on data obtained from phosphoric
433 acid digestion.

434

435 **3.2.2 Phosphoric Acid Digestion**

436

INSERT FIGURE 6

437 EFT *B. suillus* $\delta^{13}\text{C}$ enamel values ($n = 81$) average $-7.9 \pm 1.4 \text{ ‰}$ and range from -10.4

438 to -4.1 ‰ (Tables 3, S2), while $\delta^{18}\text{O}$ enamel values ($n = 81$) average $-0.8 \pm 1.2 \text{ ‰}$ and range

439 from -4.1 ‰ to 2.6 ‰ . When these samples are pooled by Collection Bay, we do not observe a

440 significant correlation between median $\delta^{13}\text{C}$ value and latitude ($p = 0.35$; Spearman's Rank

441 Correlation) or longitude ($p = 0.69$; Spearman's Rank Correlation) values at EFT (Fig. 6 A,B).

442 We do, however, recognize statistically significant differences between $\delta^{13}\text{C}$ ratio distributions (p

443 $= 0.01$, Kruskal-Wallis test of equal medians) across Collection Bays, which suggests significant

444 isotopic heterogeneity across the dune field. It is important to consider, however, that sample

445 sizes for some Bays are especially low (Table 3) and additional targeted sampling is needed to

446 further confirm these patterns.

447 We find no statistically significant differences in the mean ($p = 0.32$, ANOVA; $p = 0.32$,

448 Wilcoxon-Mann-Whitney Rank Sum Test) or variance ($p = 0.52$, F test for equal variance) of

449 $\delta^{13}\text{C}$ values between the subset of acid-etched and unetched incisors (Fig. 6C). $\delta^{13}\text{C}$ of etched

450 incisors ($n = 6$) average $-6.7 \pm 1.2 \text{ ‰}$ and range from -8.2 to -5.0 ‰ , while unetched incisors ($n =$

451 27) average $-7.4 \pm 1.2 \text{ ‰}$ and range from -10.1 to -4.1 ‰ . Additionally, we find no difference in

452 the mean ($p = 0.41$, ANOVA; $p = 0.28$, Wilcoxon-Mann-Whitney Rank Sum Test) of $\delta^{18}\text{O}$ values

453 of acid-etched and unetched incisors. We do, however, find a significant difference in the

454 variance ($p = 0.003$, F test for equal variance) in $\delta^{18}\text{O}$ values of acid-etched and unetched

455 incisors. The similarities in isotopic values between the etched and unetched specimens further

456 support the assertion that all of the EFT *B. suillus* incisors analyzed here originated from the
457 same fossil population.

458 **INSERT FIGURE 7**

459 Fossil EFT *B. suillus* incisors are significantly ($p < 0.001$, ANOVA; $p < 0.001$ Wilcoxon-
460 Mann-Whitney Rank Sum Test) enriched in $\delta^{13}\text{C}$ when compared to contemporaneous large
461 mammals ($n = 194$; Luyt et al., Lehmann et al., *In Review.*) from the site (Fig. 7). $\delta^{13}\text{C}$ values of
462 large mammals average $-10.2 \pm 1.3\text{‰}$ and range from -13.3‰ to -6.9‰ . The Lehmann et al. (*In*
463 *Review*) large mammal dataset from EFT consists of samples from taxonomically (i.e., 8
464 families) and ecologically (i.e., browsers and grazers) diverse taxa.

465

466 **3.2.3 Estimates of C₄ dietary contribution**

467 Even when considering the potential contribution of CAM vegetation, we find that the
468 mean $\delta^{13}\text{C}$ value (-7.9‰) for *B. suillus* teeth at EFT would require diets between 20 and 52% C₄
469 vegetation (Fig. 7). This is consistent with dietary estimates based upon stable isotopic analyses
470 for modern *B. suillus* obtained by Robb et al. (2012). It should be noted that the $\delta^{13}\text{C}$ values for
471 the modern mole-rats may indicate the consumption of grasses that are not native to the CFR.
472 This variable diet is consistent with descriptions of modern populations in southern Africa
473 (Bennett et al., 2009) and agrees with previous studies that indicate the presence of at least
474 some C₄ vegetation within the EFT vegetative community (Luyt et al., 2000; Lehmann et al., *In*
475 *Review*).

476

477 **3.2.4 Implications for Hominin Paleobiology**

478 The isotopic variation in the fossil *B. suillus* specimens likely reflects some variation in
479 vegetation in the past. To better understand the relationship between this variation in ancient
480 vegetation and hominin behavior we investigate the frequency of excavated artifacts at EFT and
481 the $\delta^{13}\text{C}$ signature of *B. suillus* from the various localities at EFT. We find that there is a positive

482 relationship (Kendall's Tau = 0.54; $p = 0.05$) between artifact density (count/m²) and the median
483 *B. suillus* $\delta^{13}\text{C}$ signature when binned by Collection Bay (Fig. 8). We use the non-parametric
484 Kendall's Tau correlation due to its conservative significance estimates with small sample size
485 (refer to Table 3).

486 INSERT FIGURE 8

487

488 4. Discussion

489

490 4.1 Taphonomic history of *B. suillus* at EFT

491 The taphonomic data demonstrate that at least 18% of *B. suillus* incisors from EFT
492 display evidence of digestion (i.e., acid etching), indicating that they were prey items of avian or
493 mammalian carnivores and became associated with the site through the deposition of pellets or
494 scats (Fig. 4). The $\delta^{13}\text{C}$ values from the acid-etched incisors are indistinct from $\delta^{13}\text{C}$ values of
495 teeth for which there is no evidence of acid digestion (Fig. 4C). This is also the case for $\delta^{18}\text{O}$
496 values. We conclude that the material analyzed here appears to have originated from a fossil
497 population that has a similar depositional history as the other fossils and artifacts at EFT. This
498 finding, originally suggested by Braun et al. (2013a), is supported by our analysis of the relative
499 stratigraphic abundance of *B. suillus* and large mammal fossils at EFT (Fig. 5). We note that we
500 cannot completely rule out the possibility that some of the fossil *B. suillus* material at EFT
501 represents geologically later incursions into older deposits.

502

503 4.2 Vegetative variability at EFT during the mid-Pleistocene

504 The $\delta^{13}\text{C}$ signature of *B. suillus* suggests significant vegetative variability (i.e., plants
505 utilizing the C₃, C₄ and CAM photosynthetic pathways) at EFT during the mid-Pleistocene. The
506 ubiquity of *B. suillus*, a species with high dietary flexibility (Bennett et al., 2009), at the site,

507 combined with $\delta^{13}\text{C}$ values spanning approximately 6‰ suggest the ancient local ecosystems
508 varied significantly. For comparison, the range of $\delta^{13}\text{C}$ values for *Aepyceros melampus*, a wide-
509 ranging mixed-feeding bovid, in eastern Africa is approximately 10‰ (Cerling et al., 2003). The
510 diet of *A. melampus* is directly related to the proportional representation of C_3 and C_4 vegetation
511 across ecotones, such that as these proportions change, so does the diet of *A. melampus*.
512 Thus, $\delta^{13}\text{C}$ variation in *B. suillus* from EFT is consistent with findings in modern representatives
513 (Robb et al., 2012) and suggests that the taxon was a relatively opportunistic feeder in ancient
514 times and incorporated an isotopically diverse range of vegetation into its diet.

515 Our analyses of the $\delta^{13}\text{C}$ signature of *B. suillus* (Fig. 6) suggest that the distribution of
516 vegetation at EFT was highly heterogeneous across space. The spatial distribution of vegetation
517 types at EFT could be related to highly localized landscape features (e.g., springs). The
518 heterogeneous nature of the environment at EFT, and the resources available within it, is
519 supported by the diversity of the large mammal fauna (Klein et al., 2007; Braun et al., 2013a).
520 Alternatively, the variation that we have identified may be related to the particular taphonomy of
521 this region. This is attributable to a combination of two possible factors: 1) some degree of time
522 averaging within the assemblages, and 2) a majority of *B. suillus* material originated from avian
523 pellets or mammalian scat that were deposited in locations a distance away from the area in
524 which the material was caught. Although there are clear fossil horizons at EFT (Braun et al.,
525 2013a), the depositional time represented by these horizons across the dunefield remains
526 unclear. Dynamic climatic and geologic variables may have resulted in shifting ecotones at EFT;
527 therefore a fossil sample originating from within one Collection Bay at EFT potentially
528 represents an accumulation of time-averaged sediment as is the case with almost all
529 Pleistocene archaeological sites (Shick 1987). Thus, each locality likely represents a unique
530 window into the ecosystem at a particular time in the dunefield's depositional history. Secondly,
531 predators may have transported the remains of *B. suillus* across the EFT dunefield, thus

532 decreasing the spatial fidelity of the sample. We suggest that it is likely that a combination of
533 these factors contributed to the lack of spatial patterning in the $\delta^{13}\text{C}$ signature of *B. suillus* at
534 EFT.

535

536 **4.3 Large mammals versus *Bathyergus suillus* at EFT**

537 The $\delta^{13}\text{C}$ data indicate significant dietary differences between large mammals and *B.*
538 *suillus* at EFT (Fig. 7). Based upon our dietary mixing model, even after considering the
539 potential contribution of CAM vegetation, *B. suillus* at EFT consumed significant quantities of C_4
540 vegetation. To obtain the mean EFT *B. suillus* $\delta^{13}\text{C}$ value (-7.9 ± 1.4 ‰), the diets of individual
541 mole-rats would have had to included 20 - 52% C_4 vegetation. In contrast, $\delta^{13}\text{C}$ values from
542 large mammals at EFT indicate that individuals had diets with 0-35% C_4 vegetation (Lehmann et
543 al., *In Review*), which is significantly less than that of contemporaneous *B. suillus*. This
544 comparison clearly demonstrates that mole-rat diet at EFT was different than that of large
545 mammals. Although it is difficult to assess the particular types of plants that contributed to the
546 C_4 component to *B. suillus* diets (e.g., grasses or sedges), the diet of extant *B. suillus* from the
547 CFR can potentially shed light on this issue. Although the diet of the species is especially
548 variable relative to other African mole-rat genera, more than 60% of the diet of modern *B. suillus*
549 is derived from the blades and rhizomes of *Cynodon dactylon*, a C_4 grass (Davies and Jarvis,
550 1986; Bennett and Jarvis, 1995, Smith and Winter, 1996; Yeakel et al., 2007). Although
551 *Cynodon dactylon* is not endemic to South Africa, it does suggest that *B. suillus* readily
552 consumes C_4 resources if available on the local landscape. Thus, we suggest that it seems
553 more likely that C_4 grasses and sedges, rather than CAM plants, were the primary source of
554 relatively high $\delta^{13}\text{C}$ values in *B. suillus* teeth relative to those of large mammals at EFT.

555 It is also important to consider how variation in the carbon isotope diet-tissue
556 fractionation factor ($\epsilon^*_{\text{enamel-diet}}$) affects dietary reconstructions, especially between large and
557 small mammals that potentially have different digestive physiologies (Passey et al., 2005). Here

558 we use a $\epsilon^*_{\text{enamel-diet}}$ of 11.1‰ which has been suggested appropriate for small mammals
559 (Podelsak et al., 2008). It is also important to consider, however, a scenario where $\epsilon^*_{\text{enamel-diet}}$ for
560 *B. suillus* was closer to that proposed for large mammals (i.e., 14.1‰; Cerling and Harris, 1999).
561 If the $\epsilon^*_{\text{enamel-diet}}$ for *B. suillus* were 14.1‰, then *B. suillus* at EFT during the mid-Pleistocene
562 consumed slightly greater proportions of C₄ vegetation than we suggest in Section 3.2.3 (Fig.
563 S1). Thus, the estimates provided here for the proportion of C₄ vegetation in the diet of *B.*
564 *suillus* are conservative, minimum values given uncertainties in $\epsilon^*_{\text{enamel-diet}}$ for *B. suillus* and other
565 mole-rats.

566 The carbon isotope data presented here indicate that *B. suillus* consumed significantly
567 more C₄ vegetation than large mammals at EFT in the mid-Pleistocene. We consider this to be
568 reflective of elevated concentrations of C₄ vegetation at EFT relative to the surrounding, C₃
569 vegetation dominated, CFR. Because large-bodied mammals migrate seasonally and have
570 more expansive home ranges, their isotopic signature is likely to reflect the vegetation in a
571 larger geographic region than that of *B. suillus*. Given the relatively small spatial extent of EFT
572 (~11 km²), it is likely that large mammals ranged both within and outside of site and as a result
573 incorporated vegetation from outside of the bounds of EFT. Even considering post-mortem
574 predatory transport estimates for avian predators of 1.5 km² (Colvin, 1984; Taylor, 1994), the
575 $\delta^{13}\text{C}$ data from *B. suillus* at EFT represents vegetation from a more limited geographic range
576 than that of the larger mammals, which in some cases could be greater than 50 km² (Klingel,
577 1969). It is difficult to assess the impact of mammalian carnivore predation on the distribution of
578 *B. suillus* remains at EFT, but it is unlikely that small carnivores transported mole rats far from
579 the area in which they were caught. Previous work at EFT suggests a high diversity of
580 mammalian carnivores at the site (Klein et al., 2007). Although mammalian carnivores can have
581 extensive ranges based upon body size, metabolic requirements, habitat and diet (Gittleman
582 and Harvey, 1982), our taphonomic analysis revealed that less than 20% of *B. suillus* incisors
583 showed definitive evidence of digestion. Therefore, we find it implausible that the $\delta^{13}\text{C}$ values of

584 fossil EFT *B. suillus* incisors reflect a geographic space equivalent in size to that of the home
585 range of large mammalian carnivores.

586 An additional possibility is that the C₄ component of *B. suillus* diet is related to the
587 consumption of C₄ sedges rather than C₄ grasses. Existing work by Mucina et al., (2006) and
588 Radloff et al., (2008) indicates that wetlands within the WRZ support locally abundant C₄
589 biomass. Spring features on the ancient EFT landscape could have provided the water needed
590 to fuel the growth of C₄ sedges during hot summer months in the CFR. Wetlands associated
591 with spring features could have also supported C₄ grasses and it has been demonstrated that
592 certain large ungulate taxa in the CFR preferentially target these grasses when available
593 (Radloff, 2008). If this behavior was consistent in the past, the presences of C₄ grasses at EFT
594 may have concentrated large ungulate taxa at the site and may explain the C₄ component of
595 EFT large mammal diet reported by Lehmann et al., (*In Review*). If these wetland areas,
596 however, supported only C₄ sedges, which are less likely to be consumed by large herbivores, it
597 may explain the significantly enriched $\delta^{13}\text{C}$ values of *B. suillus* relative to those of EFT large
598 mammals.

599 **4.4 C₄ vegetation in the Cape Floral Region**

600 Although the contemporary CFR lies well within the WRZ and is dominated by C₃
601 vegetation, we understand little about the evolution of this climatic system throughout the
602 Quaternary (Chase and Meadows, 2007). Previous research suggests that C₄ vegetation was
603 not a major component of CFR ecosystems at 5 Ma (Franz-Odendaal et al., 2002; Rossouw et
604 al., 2009; Dupont et al., 2011, 2013; Hoetzel et al., 2013, 2015), however analyses of enamel
605 from large mammals (Luyt et al. 2000; Hare and Sealy, 2014; Lehmann et al., *In Review*)
606 suggest a minor presence of C₄ vegetation in the mid-Pleistocene, potentially related to
607 decreased atmospheric $p\text{CO}_2$ conditions during glacial periods. Our study suggests that a C₄
608 signal within the CFR during this period may be somewhat masked by the wide-ranging nature
609 of large mammals. The carbon isotope data from *B. suillus* at EFT, which sample relatively

610 small geographic regions (<1.5 km²) indicate that some regions in the CFR potentially had
611 greater proportions of C₄ vegetation than is indicated by carbon isotope data from large
612 mammals alone.

613 It is important to consider the effect of glacial and interglacial climatic cycles on the δ¹³C
614 signatures of herbivores at EFT (Hare and Sealy, 2013). The crossover model of Ehleringer
615 (1997) and Cerling (1998) predicts that during glacial periods, atmospheric pCO₂ is lower and
616 C₄ plants should have a distinct advantage over C₃ plants. Thus, it is hypothesized that during
617 glacial periods in the CFR, C₄ vegetation would have been a more significant proportion of the
618 plant biome than during interglacial periods (Hare and Sealy, 2013). Current geochronological
619 models of EFT make it impossible to ascertain if the sediments at EFT represent a glacial or
620 interglacial period. Both large and small mammals were collected from within a single fossil- and
621 artifact-rich horizon at EFT that could represent glacial or interglacial cycles or a combination of
622 both. Regardless of the specific time period represented, EFT large and small mammals
623 represent similar depositional circumstances and were likely aggregated over a similar time
624 interval (Fig. 5).

625 Previous research has demonstrated that in addition to atmospheric pCO₂, growing
626 season temperature is the dominant climatic parameter that determines the abundance of C₄
627 vegetation within an ecosystem (Terri and Stowe, 1976; Epstein et al., 1997). These studies
628 suggest that more elevated growing season temperatures result in higher proportions of C₄
629 plants within a particular system. As with all plants, however, water availability is crucial for the
630 initiation of plant growth (Ehleringer et al., 1997). We hypothesize that the consistent presence
631 of water near springs at EFT evident from spring deposits (Braun et al., 2013a) may have
632 created conditions in which a significant proportion of C₄ vegetation could thrive during the hot,
633 dry summers of the WRZ. We further hypothesize that the prevalence of C₄ vegetation would be
634 elevated in areas with low-lying topography in close contact with the water table (i.e., spring
635 features). This relationship between spring features and elevated C₄ vegetation has been

636 demonstrated in eastern Africa (Garrett, 2015). In the contemporary CFR, increased C₄
637 biomass, specifically *Sporobolus virginicus* and *Stenotaphrum secundatum*, has been
638 documented in conjunction with estuaries and wetlands (Mucina et al., 2006; Radloff, 2008).
639 Thus, it is highly plausible that spring features and the resulting availability of water during the
640 dry summer months resulted in localized instances of C₄ vegetation at EFT during the mid-
641 Pleistocene.

642 It is also important to consider that the C₄ vegetation component of *B. suillus* enamel
643 values may have been affected by seasonal variation in the EFT ecosystem. Breeding in *B.*
644 *suillus* has been shown to be highly seasonal and tied to periods elevated rainfall (Hart et al.,
645 2006). The shorter life spans and enamel maturation periods in *B. suillus* relative to those of
646 large mammals, means that the $\delta^{13}\text{C}$ data from *B. suillus* is representative of relatively shorter
647 periods of time compared to the $\delta^{13}\text{C}$ data of large mammals at EFT. If the time of enamel
648 maturation in *B. suillus* corresponds to a seasonal period in which C₄ vegetation is more
649 abundant, then the EFT mole-rat $\delta^{13}\text{C}$ data could represent a bias towards this particular aspect
650 of the ecosystem. Carbon isotopic data from large mammals at Hodjiespunt (Hare and Sealy,
651 2013) and EFT (Lehmann et al., *In Review*) however, suggest that the differential winter rainfall
652 seen in the modern winter rainfall zone was active during the mid-Pleistocene. Thus, C₃
653 vegetation is more likely to have increased in the WRZ during instances of increased rainfall.
654 This scenario would manifest in the enamel of *B. suillus* that would reflect greater amounts of C₃
655 vegetation during these periods. This is the opposite of the pattern exhibited in the *B. suillus*
656 specimens in this study.

657 The connection between C₄ vegetation and standing water could represent an important
658 insight into the ecological mechanisms behind the elevated diversity and abundance of
659 mammalian fossils at EFT (Klein et al., 2007). The consistent presence of water would have
660 been an extremely valuable resource for animals, especially the obligate drinkers during the
661 relatively long, hot and dry summers in the WRZ. In turn, the seasonal consumption of

662 vegetation from these areas at EFT could be responsible for the small amount of C₄ vegetation
663 in the diet of large mammals from the site (Luyt et al., 2000; Lehmann et al., *In Review*).

664

665 **4.5 Implications for hominin ecology at EFT**

666 The fossil and archaeological deposits at EFT provide a rare glimpse into hominin
667 behavior between 1.0 and 0.6 Ma, a period of human history that is poorly understood in Africa
668 (Patterson et al., 2014). Previous research suggests that hominin occupation at EFT can be
669 best explained by the complex interplay of availability of stone to make artifacts and the
670 variability in food resources (Archer and Braun, 2010; Braun et al., 2013a). Our findings suggest
671 a previously undocumented diversity of vegetative resources at EFT and support this conclusion
672 on two fronts: 1) EFT likely represented a rare, resource-rich landscape within a broader
673 regional ecosystem that was relatively resource poor, and 2) this landscape presented an
674 adaptive scenario for mid-Pleistocene hominins in the Western Cape that is substantially
675 different from the summer rainfall ecosystems represented in the vast majority of similarly aged
676 deposits on the African continent.

677 Although we understand little about the position of mid-Pleistocene hominins within the
678 broader mammalian community in the CFR, EFT provides important clues into hominin
679 paleoecology during this period. Directly associated artifacts and fauna at EFT (Braun et al.,
680 2013a) suggests that hominins capitalized on meat resources and were likely drawn to EFT by
681 what may have been consistently available water and vegetation. Additionally, the incredible
682 diversity of mammalian carnivores preserved at EFT (Klein et al., 2007; Braun et al., 2013a),
683 suggests that hominins were a part of the large carnivore guild by this time, a process that
684 potentially began at least 1 million years earlier on the continent (Werdelin and Lewis, 2013).
685 Recent work by Forrest et al. (2015) suggests a higher frequency of cut marked bones which is
686 likely an underestimate due to poor bone surface preservation resulting from the Aeolian

687 depositional setting at the site, at EFT than that indicated by previous studies (Klein et al.,
688 2007).

689 The isotopic disparity between EFT *B. suillus* and EFT large mammals suggests a
690 landscape that provided hominins with locally distinct and consistent resources (i.e., water and
691 associated C₄ vegetation) during periods of resource scarcity in the broader CFR, particularly
692 during the dry summer months. Although the CFR may have been climatically dynamic during
693 the mid-Pleistocene (Chase and Meadows, 2007), we hypothesize that the resources available
694 at EFT may have provided a buffer against broader environmental, and resource instability in
695 the CFR.

696 Lastly, our analysis contributes to our understanding of intra-landscape hominin behavior
697 at EFT. Although lithic evidence indicates that hominin behavior varied in intensity across the
698 EFT dunefield (Braun et al., 2013a), we know little about the ecology of these patterns.
699 Preliminarily, our analyses suggest that the presence of C₄ resources, could have contributed to
700 this concentration. Our data indicate a positive relationship between artifact density and median
701 $\delta^{13}\text{C}$ of *B. suillus* from EFT. This finding suggests that the unique environmental conditions
702 suitable for C₄ vegetation (i.e., water during the summer months) may have also contributed to
703 the resultant discard of stone artifacts by hominin toolmakers at similar points on the landscape.
704

705 **5. Conclusion and future directions**

706 We used a large sample (n = 81) of fossil *B. suillus* incisors to assess the distribution of
707 vegetation at EFT. Our findings suggest that the paleolandscape of EFT contained a unique
708 mixture of C₄, C₃ and CAM vegetation relative to the broader fynbos-dominated C₃ ecosystem
709 of the CFR. $\delta^{13}\text{C}$ values of *B. suillus* are significantly different from those of contemporaneous
710 large mammals from EFT and suggest a plant community with a significant presence of plants
711 utilizing the C₄ photosynthetic pathway, even when the contribution of CAM vegetation in the
712 diet of *B. suillus* is considered. We hypothesize that this geographically restricted landscape

713 provided abundant resources for both hominin and non-hominin taxa and potentially buffered
714 these populations against larger environmental fluctuations and resource instability in the Cape
715 Floral Region.

716 Future studies at EFT hope to increase the resolution with which we understand both
717 hominin and large mammal behavior in the CFR. Strontium isotopic analysis of both large and
718 small mammals at the site promises to provide insight into ranging patterns and the opportunity
719 to further test many of the hypotheses presented here. In addition, geochemical sourcing of raw
720 materials utilized by EFT hominins can potentially offer insights into the utilization of regionally
721 available lithic resources (Braun et al. 2008). Lastly, increasing the chronological resolution of
722 the EFT deposits is crucial to testing climatic hypotheses, especially the impact glacial and
723 interglacial cycles on the CFR.

724

725 **Acknowledgements**

726 We would like to thank J. Sealy for valuable discussions throughout the duration of this
727 project. We thank B. Chase, A.K. Behrensmeyer, B. Passey, R. Bobe and J. Tyler Faith for
728 thoughtful input. Two anonymous reviews greatly improved the quality of this manuscript. Thank
729 you to J. Plasket and M. Shaw for fieldwork and curatorial support. We would also like to thank
730 all students on the Elandsfontein Field School (University of Cape Town, Department of
731 Archaeology). This project was made possible by NSF BCS-1219455, NSF BCS-1219494,
732 NSF-IGERT-DGE 0801634, GW Provost, GW Signature Program, the Department of Earth and
733 Planetary Sciences at Johns Hopkins University.

734

735 **Figure Captions**

736 **Figure 1.** Modern rainfall seasonality in southern Africa. Inset: location of Elandsfontein (EFT)
737 and other important archaeological locations along the west coast of southern Africa (rainfall
738 data: www.worldclim.org; Inset: modified from Braun et al., 2013a).

739

740 **Figure 2.** Temporal distribution of WCP sites. Refer to Figure 1 for spatial distribution.

741

742 **Figure 3.** A) Map of EFT Collection Bays and small mammal collection strategies. B) Shovel
743 test pit (STP) in Bay 0710; refer to Braun et al., (2013a) for further descriptions of geological
744 context of EFT; C) 0313 excavation.

745

746 **Figure 4.** A) Modern *B. suillus* skull (NMNH 344067) from Mosselbaai, South Africa; B) WCRP
747 46140 (acid etch score = 3); C) WCRP 46138 (acid etch score = 3); D) WCRP 45684 (acid etch
748 score = 0); E) WCRP 45642 (acid etch score = 2; note potential root etching); F) WCRP 45548
749 (acid etch score = 0); Arrows indicate anterior direction of specimen. Note differences in enamel
750 surface modification in 3B, 3C, 3D, 3E, 3F. 3D, 3E and 3F could be related to soil acidity,
751 microbes or both.

752

753 **Figure 5.** Altimetric analysis of the relationship between *B. suillus* fossils and large mammal
754 fossils from EFT Collection Bays. EFT *B. suillus* fossils depicted with red triangles. EFT large
755 mammal fossils depicted with black circles.

756

757 **Figure 6.** A) *B. suillus* $\delta^{13}\text{C}$ values arranged by Collection Bay from north to south, B) *B. suillus*
758 $\delta^{13}\text{C}$ values arranged by collection Bay from east to west, C) Comparison of $\delta^{13}\text{C}$ and $\delta^{18}\text{O}$
759 values of etched and unetched incisors. Center line represents the sample median, box
760 represents the 25th and 75th percentiles, whiskers represent the sample range exclusive of
761 outliers, circles represent outliers defined at 1.5 times the interquartile range.

762

763 **Figure 7.** Comparison of EFT large mammals and EFT *B. suillus*. Models of 100% C₃, CAM and
764 C₄ represent are associated with the diet of *B. suillus*, not EFT large mammals. Darker green,

765 hashed areas represent overlap between the two distributions. EFT large mammal grazer and
766 browser mean values from Lehmann et al. (*In Review*).

767

768 **Figure 8.** Relationship between Collection Bay median *B. suillus* $\delta^{13}\text{C}$ values and Bay artifact
769 density. Line represents best fit line from median *B. suillus* $\delta^{13}\text{C}$ values – artifact density linear
770 model.

771

772 **Figure S1.** $\epsilon^*_{\text{enamel-diet}}$ affect on EFT large mammal and EFT *B. suillus* distributions. A) Small
773 mammal $\epsilon^*_{\text{enamel-diet}}$ (11.1‰) following Podelsak et al., 2008, B) Large mammal $\epsilon^*_{\text{enamel-diet}}$
774 (14.1‰) following Cerling and Harris (1999).

775

776

777

778

779

780

781

782

783

784

785 **List of Tables:**

786

787 **Table 1.** Protocol used for assigning EFT *B. suillus* upper incisors to acid-etching categories

788

789 **Table 2.** $^{13}\text{C}_{\text{ε-laser-acid}}$ and $^{18}\text{O}_{\text{ε-laser-acid}}$ for EFT *Bathyergus* enamel. ^{13}C Offset¹ and ^{18}O Offset¹
790 refer to difference between values obtained in this study and those of Passey and Cerling
791 (2006)

792

793 **Table 3.** Summary of $\delta^{13}\text{C}$ and $\delta^{18}\text{O}$ EFT *B. suillus* upper incisors arranged by Collection Bay

794

795 **Table S1.** Taphonomic analysis of EFT *B. suillus* upper incisors. Refer to Table 1 for etch
796 scoring protocol.

797

798 **Table S2.** $\delta^{13}\text{C}$ and $\delta^{18}\text{O}$ values of EFT *B. suillus* upper incisors.

799

800

801

802

803

804

805

806

807

808

809

810 **Literature Cited**

811 Andrews, P., 1990. Owls, caves and fossils: predation, preservation and accumulation of small
812 mammal bones in caves, with an analysis of the Pleistocene cave faunas from
813 Westbury-sub-Mendip, Somerset, UK. University of Chicago Press. 239 pp.

814 Bar-Matthews, M., Marean, C.W., Jacobs, Z., Karkanas, P., Fisher, E.C., Herries, A.I.R., Brown,
815 K., Williams, H.M., Bernatchez, J., Ayalon, A., Nilssen, P.J., 2010. A high resolution and
816 continuous isotopic speleothem record of paleoclimate and paleoenvironment from 90 to
817 53 ka from Pinnacle Point on the south coast of South Africa. *Quaternary Science*
818 *Reviews* 29:2131-2145.

819 Behrensmeier, A.K., 2006. Climate change and human evolution. *Science* 311, 476-478.

820 Behrensmeier, A.K., Reed, K.E., 2013. Reconstructing the habitats of Australopithecus:
821 Paleoenvironments, site taphonomy, and faunas. In: Reed, K.E., Fleagle, J.G., Leakey,
822 R.E. (Eds.), *The Paleobiology of Australopithecus, vertebrate paleobiology and*
823 *paleoanthropology*. Springer, Dordrecht, Netherlands. pp. 41-60.

824 Bennett, N.C., Jarvis, J.U.M., 1995. Coefficients of digestibility and nutritional values of
825 geophytes and tubers eaten by southern African mole-rats (Rodentia; Bathyergidae).
826 *Journal of the Zoological Society, London*. 236, 189-198.

827 Bennett, N.C., Faulkes, C.G., Hart, L., Jarvis, J.U.M., 2009. *Bathyergus suillus* (Rodentia:
828 Bathyergidae). *Mammalian Species*. 828, 1-7.

829 Berger, L.R., Parkington, J.E., 1995. Brief communication: a new Pleistocene hominid-bearing
830 locality of Hoedjiespunt, South Africa. *American Journal of Physical Anthropology* 98,
831 601-609.

832 Bobe, R., Behrensmeier, A.K. 2004. The expansion of grassland ecosystems in African in
833 relation to mammalian evolution and the origin of the genus *Homo*. *Palaeogeography,*
834 *Palaeoclimatology, Palaeoecology*. 207, 399-420.

835 Boom, A., Carr, A.S., Chase, B.M., Grimes, H.L., Meadows, M.E., 2014. Leaf wax n-alkanes
836 and $\delta^{13}\text{C}$ values of CAM plants from arid southwest Africa. *Organic Geochemistry*. 67,
837 99-102.

838 Braun, D.R., Levin, N.E., Stynder, D., Herries, A.I.R., Archer, W., Forrest, F., Roberts, D.L.,
839 Bishop, L.C., Matthews, T., Lehmann, S.B., Pickering, R., Fitzsimmons, K.E., 2013a.

840 Mid-Pleistocene hominin occupation at Elandsfontein, Western Cape, South Africa.
841 Quaternary Science Reviews. 82, 145-166.

842 Braun, D.R., Levin, N.E., Roberts, D., Stynder, D., Forrest, F., Herries, A.I., Matthews, T.,
843 Bishop, L., Archer, W., Pickering, R. 2013b. Initial investigations of Acheulean hominin
844 behavior at Elandsfontein. In: Jerardino, A., Malan, A., Braun, D.R. (Eds.). The
845 Archaeology of the West Coast of South Africa. Archaeopress. pp. 10-23.

846 Brown, K.S., Marean, C.W., Herries, A.I.R., Jacobs, Z., Tribolo, C., Braun, D.R., Roberts, D.L.,
847 Meyer, M.C., Bernatchez, J., 2009. Fire as an engineering tool in early modern humans.
848 Science. 325, 859-862.

849 Carr, A.S., Thomas, D.S.G., Bateman, M.D., Meadows, M.E., Chase, B., 2006. Late Quaternary
850 paleoenvironments in the winter-rainfall zone of southern Africa: palynological and
851 sedimentological evidence from the Agulhas Plain. Palaeogeography,
852 Palaeoclimatology, Palaeoecology. 239, 147-165.

853 Cerling, T.E. and Harris, J.M., 1999. Carbon isotope fractionation between diet and bioapatite in
854 ungulate mammals and implications for ecological and paleoecological studies.
855 Oecologia 120, 347-363.

856 Cerling, T.E., Harris, J.M., Passey, B.H., 2003. Diets of East African Bovidae based upon stable
857 isotope analysis. Journal of Mammalogy. 84:456-470.

858 Chase, B.M., Meadows, M.E., 2007. Late Quaternary dynamics of southern Africa's winter
859 rainfall zone. Earth-Science Reviews. 84, 103-138.

860 Colvin, B.A., 1984. Barn owl foraging behavior and secondary poisoning hazard from
861 rodenticide use on farms. Ph.D. Thesis. Bowling Green State University.

862 Cowling, R., 1992. Fynbos: South Africa's unique floral kingdom. University of Cape Town
863 Press, Cape Town. 156 pp.

864 Davies, K.C., Jarvis, J.U.M., 1986. The burrow systems and burrowing dynamics of the mole-
865 rats *Bathyergus suillus* and *Cryptomys hottentotus* in the fynbos of the south-western
866 Cape, South Africa. *Journal of Zoology*. 209, 125-147.

867 Deacon, H.J., 1998. Elandsfontein and Klasies river revisited. In: Ashton, N., Healy, F., Pettitt,
868 P.B. (Eds.). *Stone Age Archaeology: Essays in Honour of John Wymer*. Oxbow Books,
869 Oxford, pp. 23-28.

870 deMenocal, P.B., 2004. African climate change and faunal evolution during the Pliocene-
871 Pleistocene. *Earth and Planetary Science Letters* 220, 3-24.

872 Dietl, H., Kandal, A.W., Conard, N.J., 2005. Middle Stone Age settlement and landuse at the
873 open-air sites of Geelbek and Anyskop, South Africa. *Journal of African Archaeology* 3,
874 233-244.

875 Drennan, M.R., 1953. The Saldanha skull and its associations. *Nature* 172, 791-793.

876 Dupont, L., 2011. Orbital scale vegetation change in Africa. *Quaternary Science Reviews* 30,
877 3589-3602.

878 Dupont, L.M., Rommerskirchen, F., Mollenhauer, G., Schefuß, 2013. Miocene to Pliocene
879 changes in South African hydrology and vegetation in relation to the expansion of C₄
880 plants. *Earth and Planetary Science Letters* 375, 408-417.

881 Ehleringer, J.R., Cerling, T.E., Helliker, B.R., 1997. C₄ photosynthesis, atmospheric CO₂, and
882 climate. *Oecologia*. 112, 285-299.

883 Epstein, H.E., Lauenroth, W.K., Burke, I.C., Coffin, D.P., 1997. Productivity patterns of C₃ and
884 C₄ functional types in the U.S. Great Plains. *Ecology*. 78, 722-731.

885 Faith, J.T., 2011. Ungulate community richness, grazer extinctions, and human subsistence
886 behavior in southern Africa's Cape Floral Region. *Palaeogeography, Palaeoclimatology,*
887 *Palaeoecology* 306:219-227.

888 Faith, J.T., Behrensmeyer, A.K., 2013. Climate change and faunal turnover: testing the
889 mechanics of the turnover-pulse hypothesis with South African fossil data. *Paleobiology*
890 39:609-627.

891 Faith, J.T., Tryon, C.A., Peppe, D.J., Beverly, E.J., Blegen, N., Blumenthal, S., Chritz, K.,
892 Driese, S.G., Patterson, D.B., 2015. Paleoenvironmental context of the Middle Stone
893 Age record from Karungu, Lake Victoria Basin, Kenya, and its implications for human
894 and faunal dispersal in East Africa. *Journal of Human Evolution* 83:28-45.

895 Feakins, S.J., Levin, N.E., Liddy, H.M., Sieracki, A., Eglinton, T.I., Bonnefille, R., 2013.
896 Northeast African vegetation change over 12 m.y. *Geology*. 41, 295-298.

897 Fernandez-Jalvo, Y., Andrews, P., 1992. Small mammal taphonomy of Gran Dolina, Atapuerca
898 (Burgos), Spain. *Journal of Archaeological Science*. 19, 407-428.

899 Fernandez-Jalvo, Y. 1995. Small mammal taphonomy at La Trinchera de Atapuerca (Burgos,
900 Spain): A remarkable example of taphonomic criteria used for stratigraphic correlation's
901 and palaeoenvironmental interpretations. *Paleogeography, Paleoclimatology,*
902 *Paleoecology* 114:167-195.

903 Forrest, F.L., Stynder, D.D., Bishop, L.C., Levin, N.E., Matthews, T., Braun, D.R., 2015.
904 Zooarchaeological analysis of newly excavated Middle Pleistocene deposits from
905 Elandsfontein, South Africa. *Paleoanthropology Annual Meeting Abstracts*. San
906 Francisco, CA.

907 Franz-Odenhall, T.A., Lee-Thorp, J.A., Chinsamy, A., 2002. New evidence for the lack of C4
908 grassland expansion during the early Pliocene at Langebaanweg, South Africa.
909 *Paleobiology*. 28, 378-388.

910 Garrett, N.D., Fox, D.L., McNulty, K.P., Tryon, C.A., Faith, J.T., Peppe, D.J., Van Plantinga, A.,
911 2015. Stable isotope paleoecology of late Pleistocene Middle Stone Age humans from
912 equatorial East Africa, Lake Victoria Basin, Kenya. *Journal of Human Evolution*. 82:1-14.

913 Gittleman, J.L., Harvey, P.H., 1982. Carnivore home-range size, metabolic needs and ecology.
914 Behavioral Ecology and Sociobiology. 10:57-63.

915 Hare, V., Sealy, J., 2013. Middle Pleistocene dynamics of southern Africa's winter rainfall zone
916 $\delta^{13}\text{C}$ and $\delta^{18}\text{O}$ values of Hoedjiespunt faunal enamel. Palaeogeography,
917 Palaeoclimatology, Palaeoecology. 374, 72-80.

918 Hart, L., O'Riain, M.J., Jarvis, J.U.M., Bennett, N.C., 2006. Is the Cape Dune mole-rat, *B. suillus*
919 (Rodentia: Bathyergidae), a seasonal or aseasonal breeder? Journal of Mammalogy 87,
920 1078-1085.

921 Henshilwood, C.S., 1997. Identifying the collector: Evidence for human processing of the Cape
922 Dune Mole-rat, *Bathyergus suillus*, from Blombos Cave, Southern Cape, South Africa.
923 Journal of Archaeological Science. 24, 659-662.

924 Henshilwood, C.S., d'Errico, F., Yates, R., Jacobs, Z., Tribolo, C., Duller, G.A.T., Mercier, N.,
925 Sealy, J.C., Valladas, H., Watts, I., Wintle, A.G., 2002. Emergence of modern human
926 behavior: middle stone age engravings from South Africa. Science. 285, 1278-1280.

927 Herbst, M., Jarvis, J.U.M., Bennett, N.C., 2004. A field assessment of reproductive seasonality
928 in the threatened wild Namaqua dune mole-rat (*Bathyergus janetta*). Journal of Zoology.
929 263, 259-268.

930 Herries, A.I.R., Pickering, R., Adams, J.W., Curnoe, D., Warr, G., Latham, A.G., Shaw, J., 2013.
931 A multi-disciplinary perspective on the age of Australopithecus in southern Africa: In:
932 Reed, K.E., Fleagle, J.G., Leakey, R.E. (Eds.), The Paleobiology of Australopithecus,
933 vertebrate paleobiology and paleoanthropology. Springer, Dordrecht, Netherlands, pp.
934 21-40.

935 Hoetzel, S., Dupont, L., Schefuß, E., Rommerskirchen, F., Wefer, G., 2013. The role of fire in
936 Miocene to Pliocene C₄ grassland and ecosystem evolution. Nature Geoscience. 6,
937 1027-1030.

938 Hoetzel, S., Dupont, L.M., Wefer, G., 2015. Miocene-Pliocene vegetation change in south-
939 western Africa (ODP Site 1081, offshore Namibia). *Palaeogeography,*
940 *Palaeoclimatology, Palaeoecology.* 423, 102-108.

941 Klein, R.G., 1983. Palaeoenvironmental implications of Quaternary large mammals in the fynbos
942 region. In: Deacon, H.J., Hendley, Q.B., Lambrechts, J.J.N. (Eds.) *Fynbos*
943 *Palaeoecology* A Preliminary Synthesis. South African National Scientific Programmes,
944 Report 75, Pretoria. pp. 116-138.

945 Klein, R.G., 1988. Archaeological significance of animal bones from Acheulean sites in southern
946 Africa. *African Archaeological Review.* 6, 3-25.

947 Klein, R.G., 1991. Size variation in the Cape Dune Molerat (*Bathyergus suillus*) and late
948 Quaternary climatic change in Southwestern Cape Province, South Africa. *Quaternary*
949 *Research.* 36, 243-256.

950 Klein, R.G., Avery, G., Cruz-Uribe, K., Steele, T.E., 2007. The mammalian fauna associated
951 with an archaic hominin skullcap at later Acheulean artifacts at Elandsfontein, Western
952 Cape Province, South Africa. *Journal of Human Evolution.* 52, 164-186.

953 Klingel, H., 1969. Reproduction in the plains zebra, *Equus burchelli boehmi*: behaviour and
954 ecological factors. *Journal of Reproduction and Fertility,* 6, 339-345.

955 Kohn, M.J., 2010. Carbon isotope compositions of terrestrial C3 plants as indicators of
956 (paleo)ecology and (paleo)climate. *Proceedings of the National Academy of Sciences*
957 107:19691-19695.

958 Lehmann et al., (*In Review.*) Stable isotopic composition of fossil mammal teeth and
959 environmental change in southwestern South Africa during the Pliocene and
960 Pleistocene. *Palaeogeography, Palaeoclimatology, Palaeoecology.*

961 Levin, N.E., 2015. Environment and climate of early human evolution. *Annual Review of Earth*
962 *and Planetary Sciences* 43, 405-429.

963 Luyt, J., Lee-Thorp, J., Avery, G., 2000. New light on middle Pleistocene west coast
964 environments from Elandsfontein, western Cape, South Africa. *South African Journal of*
965 *Science*. 96, 399-403.

966 Marean, C.W., Bar-Matthews, M., Bernatchez, J., Fisher, E., Goldberg, P., Herries, A.I.R.,
967 Jacobs, Z., Jerardino, A., Karkanas, P., Minichillo, T., Nilssen, P.J., Thompson, E.,
968 Watts, I., Williams, H.M., 2007. Early human use of marine resources and pigment in
969 South Africa during the Middle Pleistocene. *Nature*. 449, 905-908

970 Marean, C.W., 2010. Pinnacle Point Cave 13B (Western Cape Province, South Africa) in
971 context: The Cape Floral kingdom, shellfish, and modern human origins. *Journal of*
972 *Human Evolution*. 59, 425-443.

973 Maslin, M.A., Pancost, R.D., Wilson, K.E., Lewis, J., Trauth, M.H., 2012. Three and a half million
974 year history of moisture availability of South West Africa: Evidence from ODP site 1085
975 biomarker records. *Palaeogeography, Palaeoclimatology, Palaeoecology* 317-318, 41-
976 47.

977 Matthews, T., 2002. South African micromammals and predators: some comparative results.
978 *Archaeometry*. 44, 363-370.

979 Matthews, T., Denys, C., Parkington, J.E., 2005. The palaeoecology of the micromammals from
980 the late middle Pleistocene site of Hoedjiespunt 1 (Cape Province, South Africa). *Journal*
981 *of Human Evolution* 49, 432-451.

982 Matthews, T., 2006a. Taphonomic characteristics of micromammals predated by small
983 mammalian carnivores in South Africa: applications to the fossil record. *Journal of*
984 *Taphonomy*. 4, 143-161.

985 Matthews, T., Parkington, J.E., Denys, C., 2006b. The taphonomy of the micromammals from
986 the late Middle Pleistocene site of Hoedjiespunt 1 (Cape Province, South Africa). *Journal*
987 *of Taphonomy* 4:11-26

988 McBrearty, S., Brooks, A.S., 2000. The revolution that wasn't: a new interpretation of the origin
989 of modern human behavior. *Journal of Human Evolution* 39, 453-463.

990 Mucina, L., Rutherford, M.C., Powrie, L.W., 2006. Vegetation atlas of South Africa, Lesotho and
991 Swaziland. Mucina, L., Rutherford, M.C. (Eds.). *The vegetation of South Africa, Lesotho*
992 *and Swaziland*. South African National Biodiversity Institute, Pretoria. pp. 748-790.

993 Passey, B.H., Robinson, T.F., Ayliffe, L.K., Cerling, T.E., Sponheimer, M., Dearing, M.D.,
994 Roeder, B.L., Ehleringer, J.R., 2005. Carbon isotope fractionation between diet, breath
995 CO₂, and bioapatite in different mammals. *Journal of Archaeological Science* 32:1459-
996 1470.

997 Passey, B.H., Cerling, T.E., 2006. In situ stable isotope analysis ($\delta^{13}\text{C}$, $\delta^{18}\text{O}$) of very small teeth
998 using laser ablation GC/IRMS. *Chemical Geology*. 235, 238-249.

999 Patterson, D.B., Faith, J.T., Bobe, R., Wood, B., 2014. Regional diversity patterns in African
1000 bovids, hyaenids, and felids during the past 3 million years: the role of taphonomic bias
1001 and implications for the genus *Paranthropus*. *Quaternary Science Reviews*. 96, 9-22.

1002 Peters, C.R., Vogel, J.C., 2005. Africa's wild plant foods and possible early hominid diets.
1003 *Journal of Human Evolution*. 48, 219-236.

1004 Pickering, R., Kramers, J.D., Hancox, P.J., de Ruiter, D.J., Woodhead, J.D., 2011.
1005 Contemporary flowstone development links early hominin bearing cave deposits in South
1006 Africa. *Earth and Planetary Letters*. 306, 23-32.

1007 Podlesak, D.W., Torregrossa, A., Ehleringer, J.R., Dearing, M.D., Passey, B.H., Cerling, T.E.,
1008 2008. Turnover of oxygen and hydrogen isotopes in the body water, CO₂, hair, and
1009 enamel of a small mammal. *Geochimica et Cosmochimica Acta*. 72, 19-35.

1010 Potts, R., 1998. Variability selection and hominid evolution. *Evolutionary Anthropology*. 7, 81-96.

1011 Radloff, F.G.T., 2008. The ecology of large herbivores native to the coastal lowlands of the
1012 Fynbos Biome in the Western Cape, South Africa. Doctoral Dissertation, Department of
1013 Botany, University of Stellenbosh, South Africa.

- 1014 Rick, T.C. 2002. Eolian processes, ground cover, and the archaeology of coastal dunes: a
1015 taphonomic case study from San Miguel Island, California, USA. *Geoarchaeology*
1016 17:811-833.
- 1017 Rebelo, A.G., Boucher, C., Helme, N., Mucina, L., Rutherford, M.C., 2006. Fynbos biome. In:
1018 Mucina, L., Rutherford, M.C., (Eds.). *The vegetation of South Africa, Lesotho, and*
1019 *Swaziland*. South African National Biodiversity Institute. Pretoria. pp. 52-219.
- 1020 Reed, D.N., 2007. Serengeti micromammals and their implications for Olduvai
1021 paleoenvironments. In: Bobe, R., Alemseged, Z., Behrensmeyer, A.K., (Eds.). *Hominn*
1022 *environments in the East African Pliocene: An assessment of the faunal evidence*.
1023 Springer, Dordrecht, Netherlands. pp. 217-256.
- 1024 Robb, G.N., Woodborne, S., Bennett, N.C., 2012. Subterranean sympatry: An investigation into
1025 diet using stable isotope analysis. *PLoS ONE*. 7, e48572.
- 1026 Rossouw, L., Stynder, D., Haarhof, P., 2009. Evidence for opal phytolith preservation in the
1027 Langebaanweg 'E' Quarry Varswater Formation and its potential for paleohabitat
1028 reconstruction. *South African Journal of Science* 105, 223-227.
- 1029 Shick, K.D., 1987. Modeling the formation of Early Stone Age artifact concentrations. *Journal of*
1030 *Human Evolution* 16:789-807.
- 1031 Skead, C.J., 1980. *Historical mammal incidence in the Cape Province, Volume I*. Department of
1032 *Nature and Environmental Conservation of the Provincial Administration of the Cape of*
1033 *Good Hope, Cape Town*.
- 1034 Singer, R., 1961. The new fossil sites from Langebaanweg, South Africa. *Current Anthropology*
1035 2, 385-387
- 1036 Singer, R., Heltne, P.G., 1966. Further notes on a bone assemblage from Hopefield, South
1037 Africa. *Museo Arqueológico*. pp. 261-264.
- 1038 Singer, R., Wymer, J., 1968. Archaeological investigations at the Saldanha skull site in South
1039 Africa. *South African Archaeological Bulletin*. 23, 63-74.

1040 Smith, J.A.C., Winter, K., 1996. Taxonomic distribution of Crassulacean acid metabolism. In:
1041 Winter, K., Smith, J.A.C., (Eds.). Crassulacean acid metabolism: biochemistry,
1042 ecophysiology, and evolution. Springer, Berlin. pp. 427-436.

1043 Stynder, D., 2009. The diets of ungulates from the hominid fossil-bearing site of Elandsfontein,
1044 Western Cape, South Africa. Quaternary Research 71, 62-70.

1045 Taylor, I., 1994. Barn Owls. Cambridge University Press. Cambridge.

1046 Terri, J.A., Stowe, L.G., 1976. Climatic patterns and the distribution of C₄ grasses in North
1047 America. Oecologia 23, 1-12.

1048 Terry, R.C., 2007. Inferring predator identity from skeletal damage of small-mammal prey
1049 remains. Evolutionary Ecology Research. 9, 199-219.

1050

1051 Tieszen, L.L., Senyimba, M.M., Imbamba, S.K., Troughton, J.H., 1979. The distribution of C₃
1052 and C₄ grasses along an altitudinal and moisture gradient in Kenya. Oecologia 37, 337-
1053 350.

1054 Tryon, C.E., Faith, J.T., Peppe, D.J., Keegan, W.F., Jenkins, K.H., Nightingale, S., Patterson,
1055 D., Van Platinga, A., Driese, S., Johnson, C.R., Beverly, E.J., 2014. Sites on the
1056 landscape: paleoenvironmental context of late Pleistocene archaeological sites from the
1057 Lake Victoria basin, equatorial East Africa. Quaternary International. 331, 20-30.

1058 Tryon, C.A., Crevecoeur, I., Faith, J.T., Ekshtain, R., Nivens, J., Patterson, D.B., Mbua, E.,
1059 Spoor, F. (2015) Late Pleistocene age and archaeological context for the hominin
1060 calvaria from GvJm-22 (Lukenya Hill, Kenya). Proceedings of the National Academy of
1061 Sciences 112:2682-2687.

1062 Van Daele, P.A.A.G., Faulkes, C.G., Verheyen, E., Adriaens, D., 2007. African mole-rats
1063 (Bathyergidae): A complex radiation in tropical soils. In: Begall, S., Burda, H., Schleich,
1064 C.E., (Eds.). Subterranean Rodents: News from Underground. Springer-Verlag, Berlin.
1065 pp. 357-373.

1066 Vogel, J.C., Fuls, A., Ellis, R.P., 1978. The geographical distribution of Kranz grasses in South
1067 Africa. *South African Journal of Science*. 74:209-215.

1068 Volman, T.P., 1978. Early archaeological evidence for shellfish collecting. *Science* 201, 911-
1069 913.

1070 Vrba, E., 1995. The fossil record of African antelopes (Mammalia, Bovidae) in relation to human
1071 evolution and paleoclimate. In: Vrba, E., Denton, G., Burkle, L., Partridge, T., (Eds.)
1072 *Paleoclimate and Evolution with Emphasis on Human Origins*, Yale University Press,
1073 New Haven, CT. pp. 385-424.

1074 Yeakel, J.D., Bennett, N.C., Koch, P.L., Dominy, N.J., 2007. The isotopic ecology of mole rats
1075 informs hypotheses on the evolution of human diet. *Proceedings: Biological Sciences*.
1076 274, 1723-1730.

1077

1078

Figure 1. Modern rainfall seasonality in southern Africa. Inset: location of Elandsfontein (EFT) and other important archaeological locations along the west coast of southern Africa (rainfall data: www.worldclim.org; Inset: modified from Braun et al., 2013a).

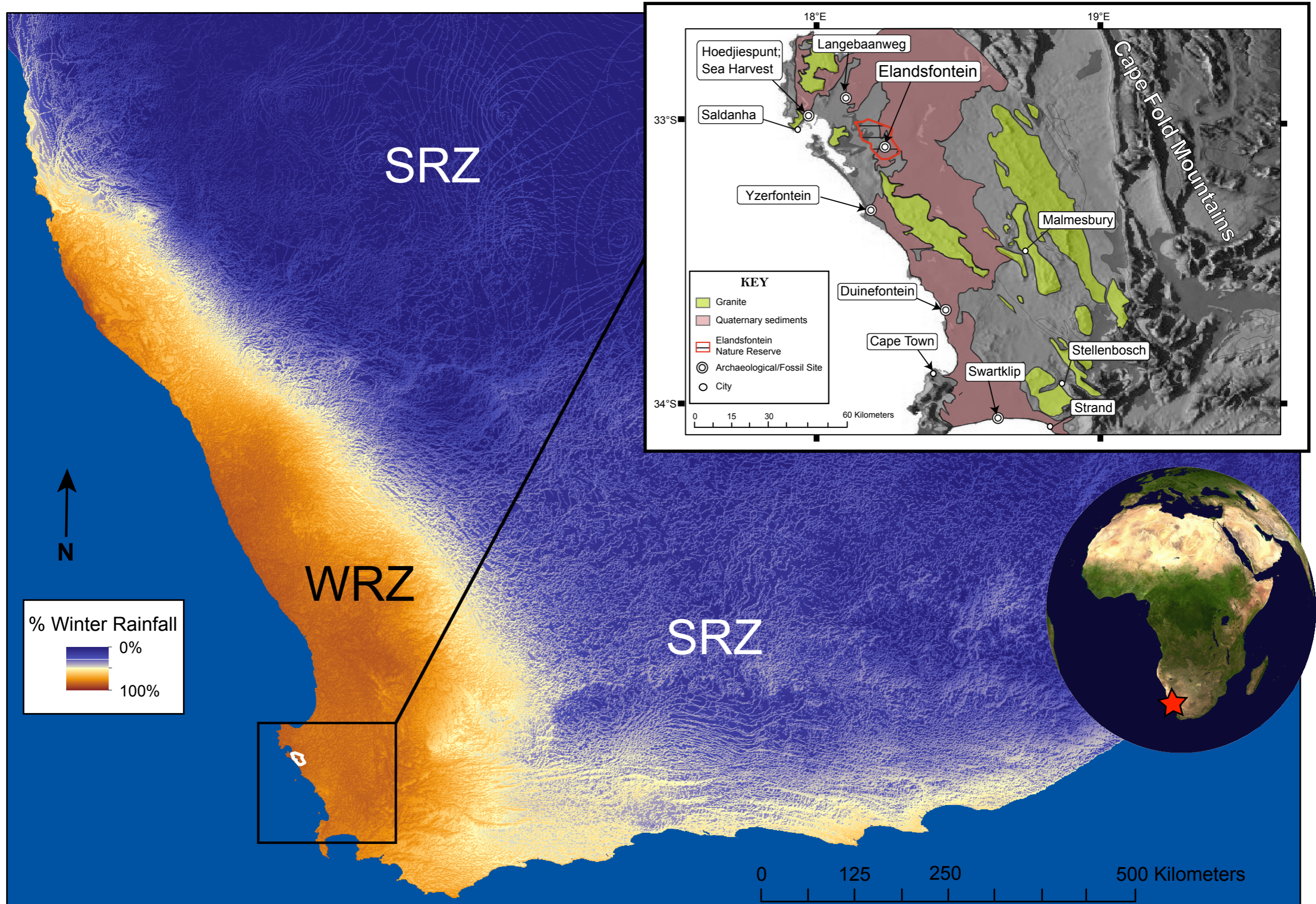


Figure 2. Temporal distribution of WCP sites. Refer to Figure 1 for spatial distribution.

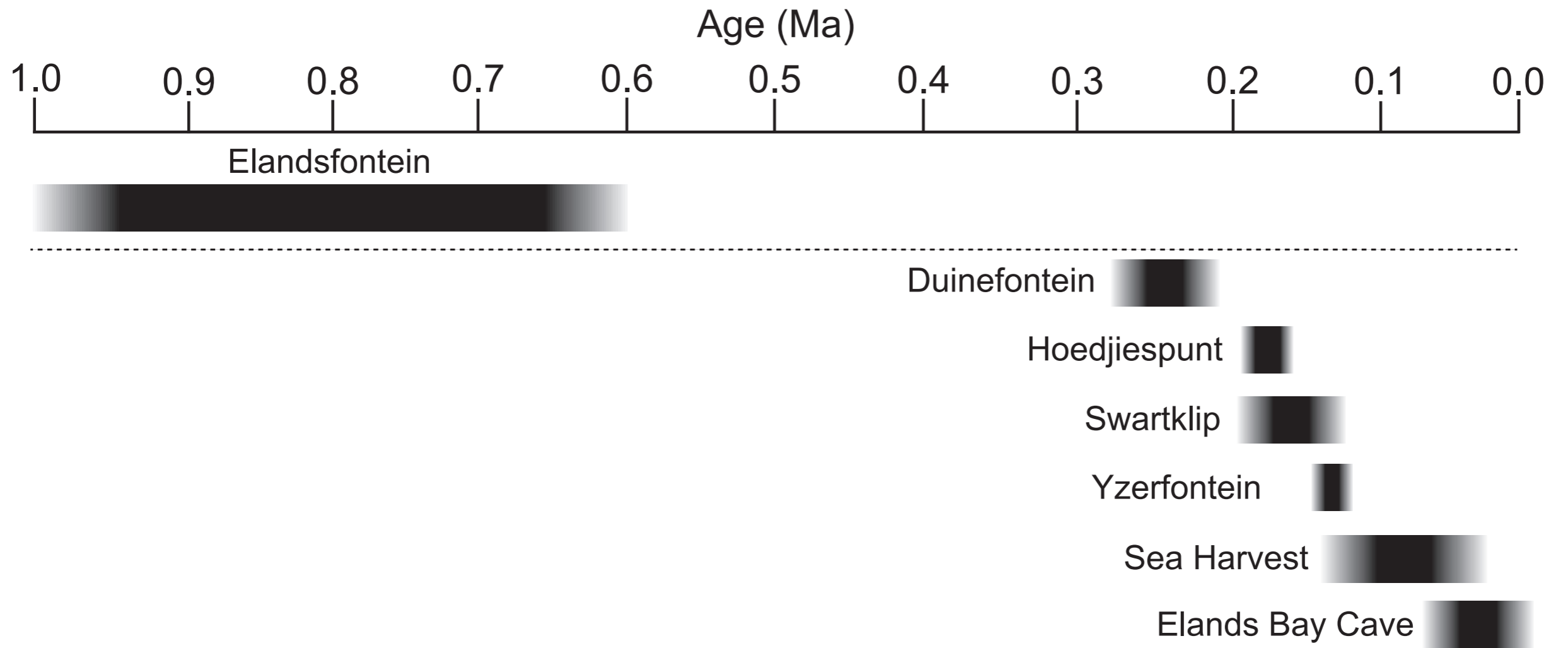
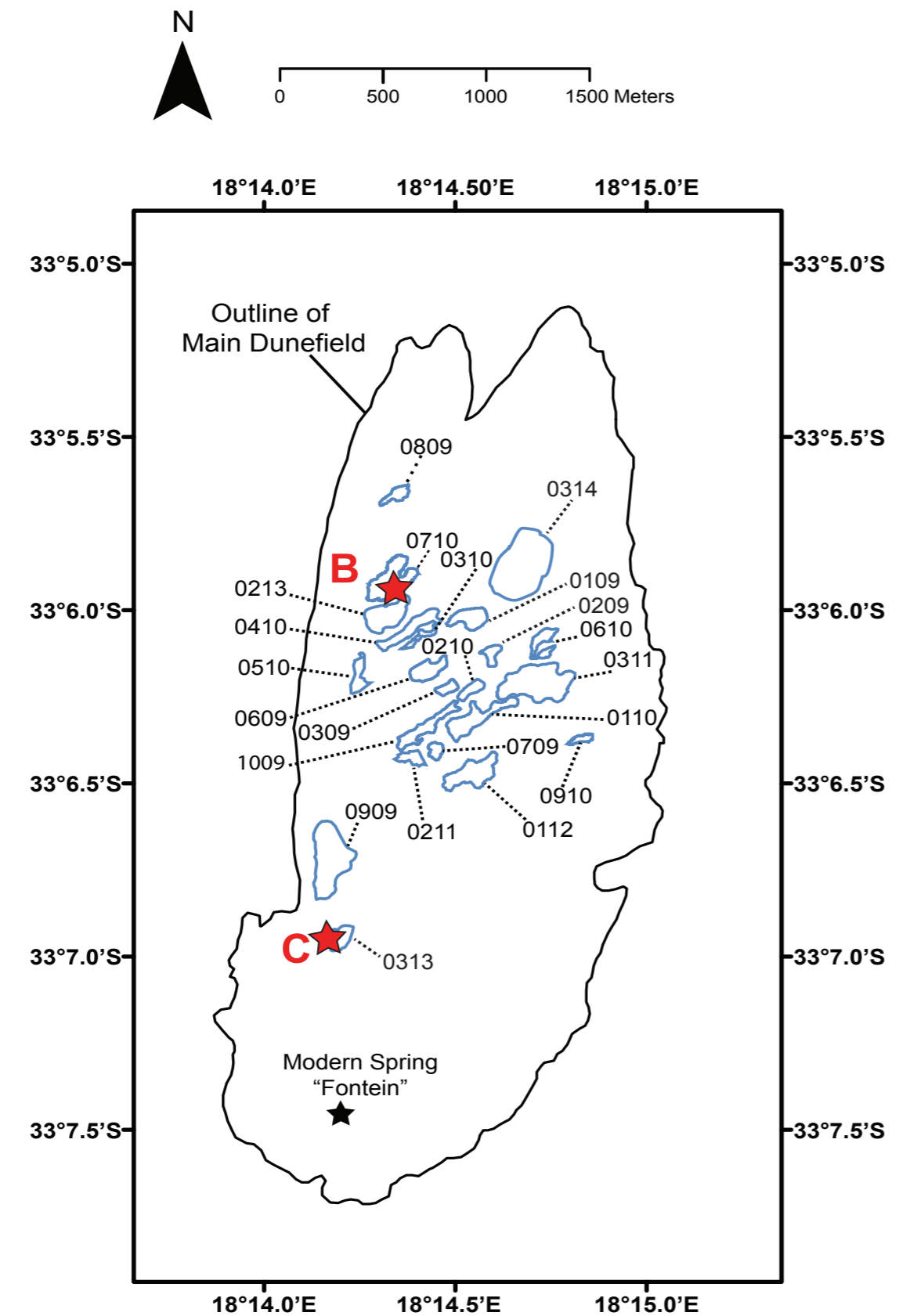


Figure 3. A) Map of EFT Collection Bays and small mammal collection strategies. B) Shovel test pit (STP) in Bay 0710; refer to Braun et al., (2013a) for further descriptions of geological context of EFT; C) 0313 excavation.



A.

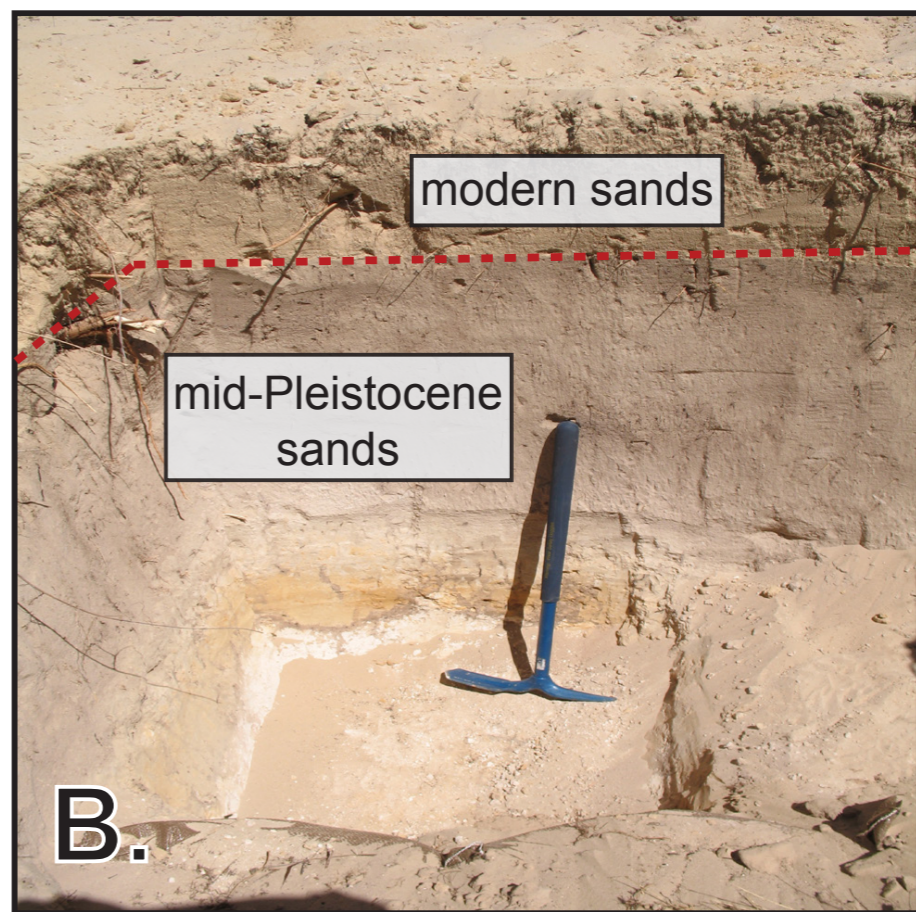


Figure 4. A) Modern *B. suillus* skull (NMNH 344067) from Mosselbaai, South Africa; B) WCRP 46140 (acid etch score = 3); C) WCRP 46138 (acid etch score = 3); D) WCRP 45684 (acid etch score = 0); E) WCRP 45642 (acid etch score = 2; note potential root etching); F) WCRP 45548 (acid etch score = 0); Arrows indicate anterior direction of specimen. Note differences in enamel surface modification in 3B, 3C, 3D, 3E, 3F. 3D, 3E and 3F could be related to soil acidity, microbes or both.

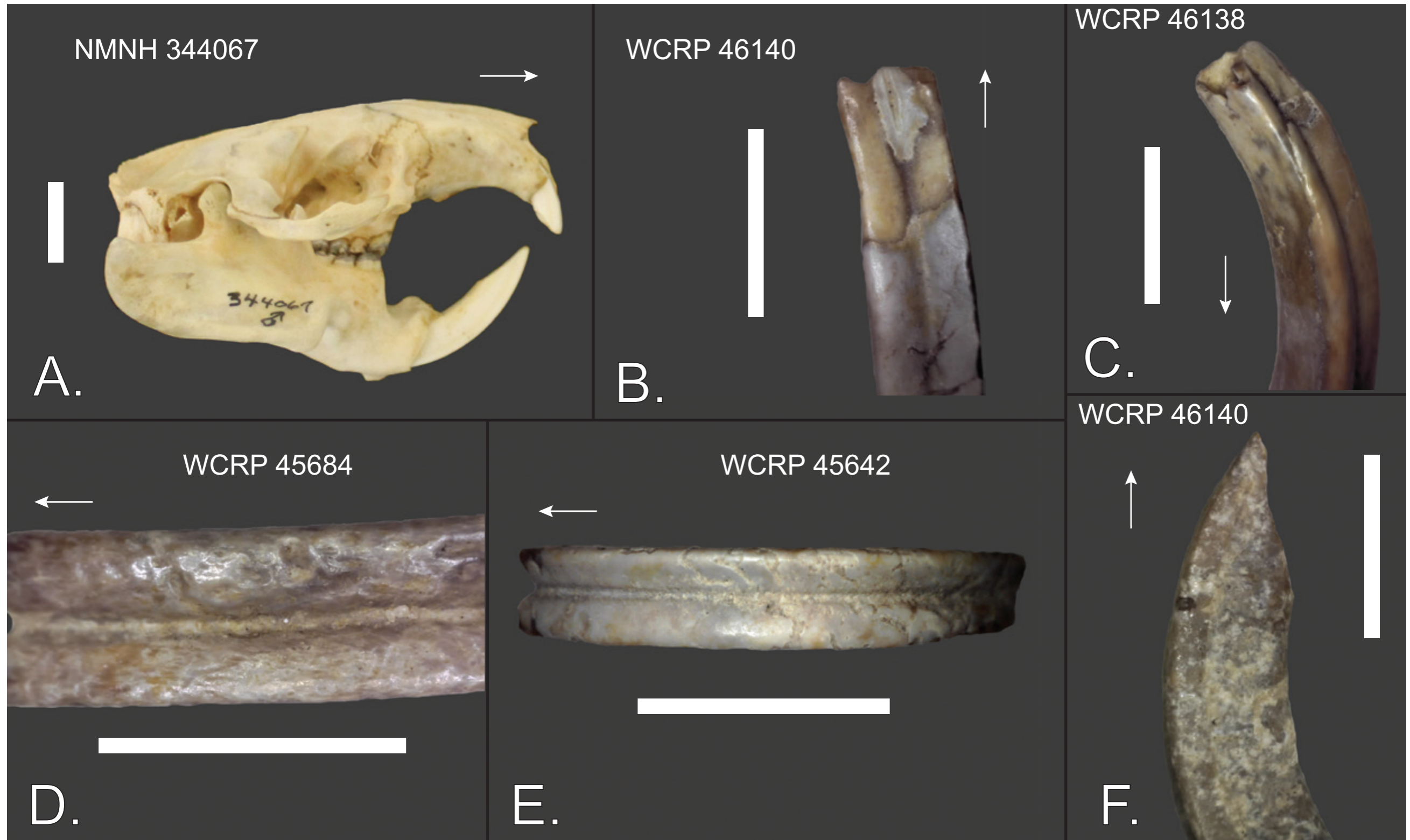


Figure 5. Altimetric analysis of the relationship between *B. suillus* fossils and large mammal fossils from EFT Collection Bays. EFT *B. suillus* fossils depicted with red triangles. EFT large mammal fossils depicted with black circles.

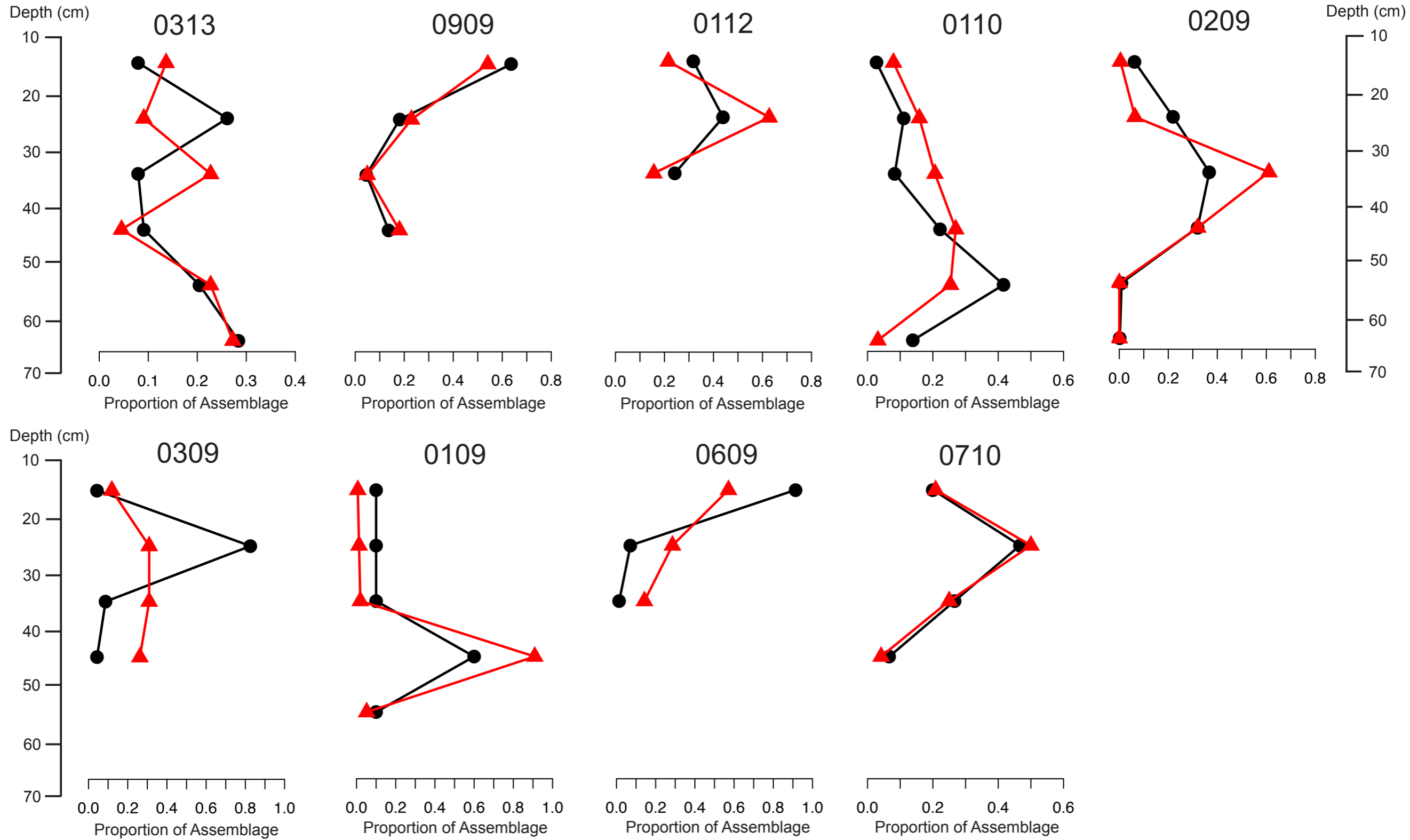


Figure 6. A) *B. suillus* $\delta^{13}\text{C}$ values arranged by Collection Bay from north to south, B) *B. suillus* $\delta^{13}\text{C}$ values arranged by collection Bay from east to west, C) Comparison of $\delta^{13}\text{C}$ and $\delta^{18}\text{O}$ ratios of etched and unetched incisors. Center line represents the sample median, box represents the 25th and 75th percentiles, whiskers represent the sample range exclusive of outliers, circles represent outliers defined at 1.5 times the interquartile range.

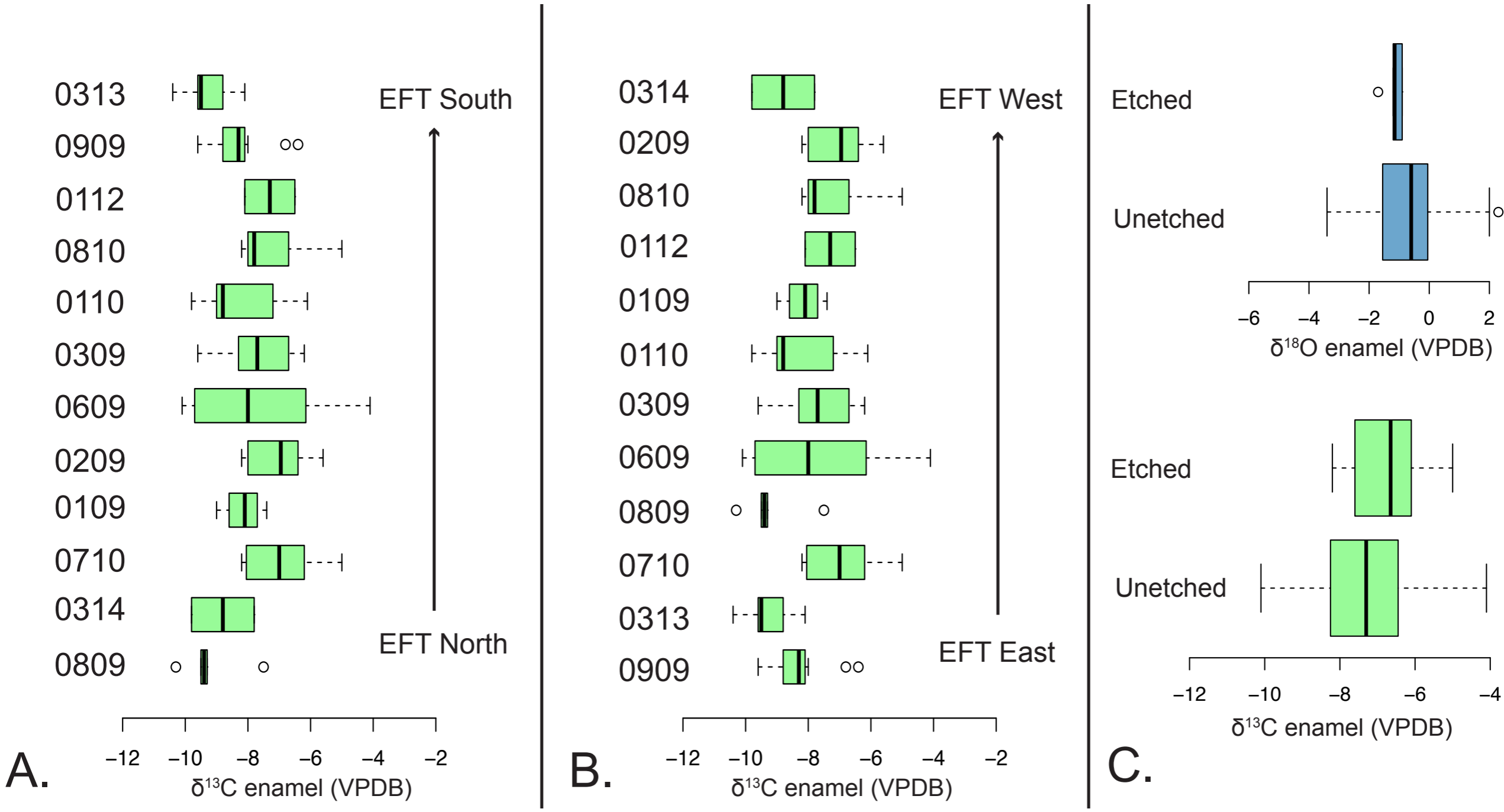


Figure 7. Comparison of EFT large herbivores and EFT *B. suillus*. 100% C₃, CAM and C₄ represent are associated with the diet of *B. suillus*, not EFT large herbivores. Darker green, hashed areas represent overlap between the two distributions. EFT large mammal grazer and browser mean values from Lehmann et al. (*In Review*).

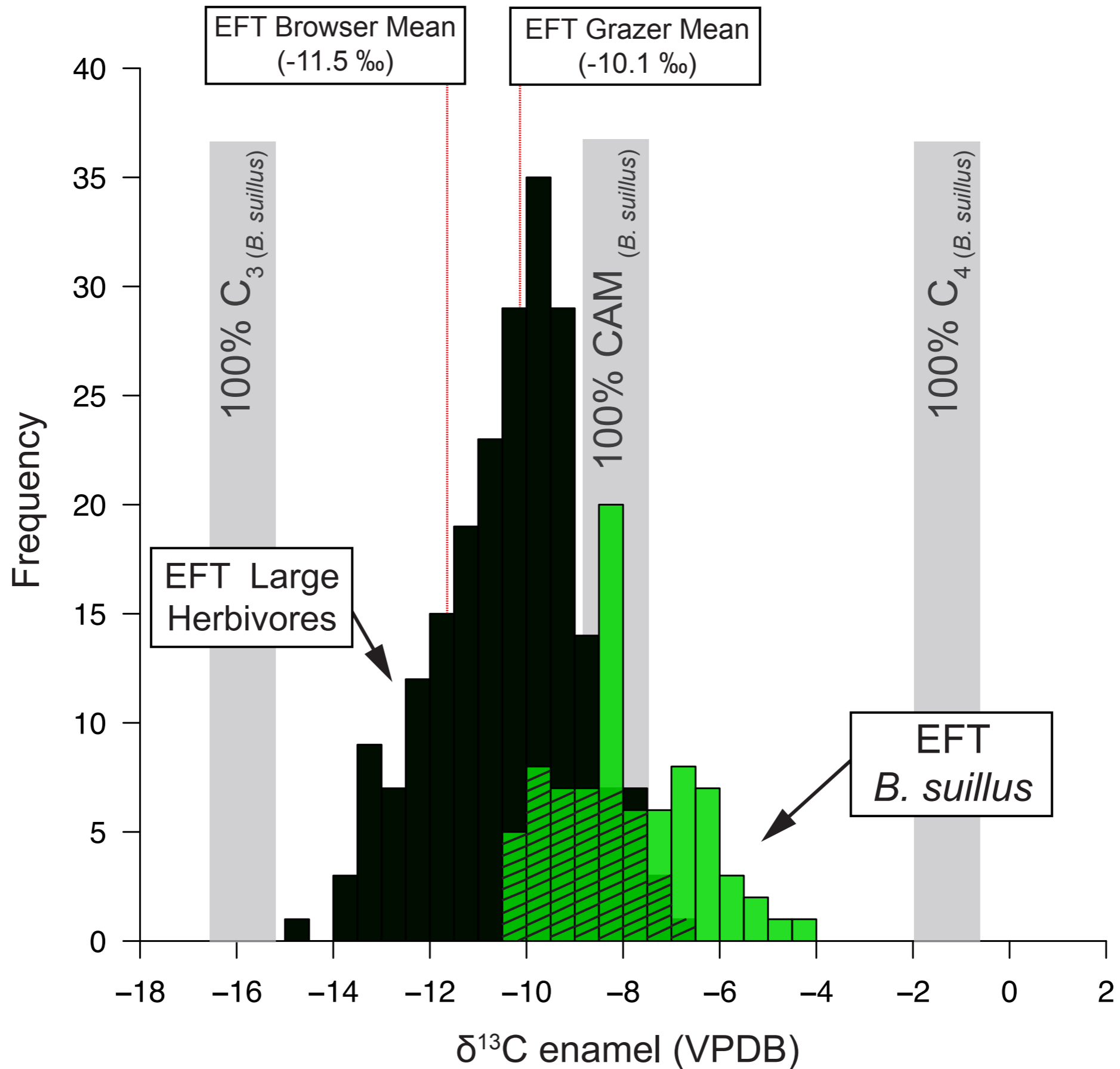


Figure 8. Relationship between Collection Bay median *B. suillus* $\delta^{13}\text{C}$ values and Bay artifact density. Line represents best fit line from median *B. suillus* $\delta^{13}\text{C}$ values – artifact density linear model.

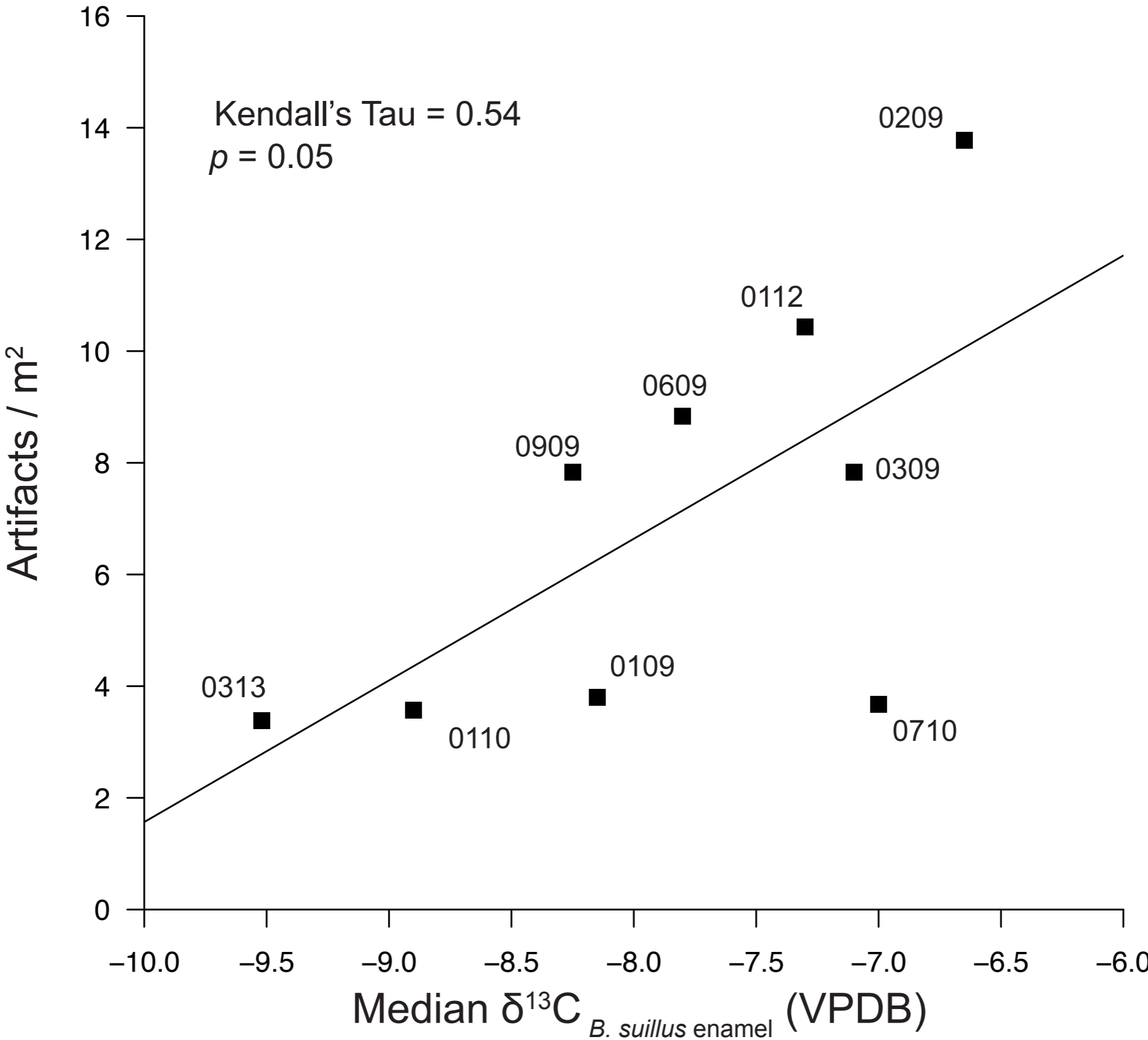


Figure S1. $\epsilon^*_{\text{enamel-diet}}$ effect on EFT large herbivore and EFT *B. suillus* distributions. A) Small mammal $\epsilon^*_{\text{enamel-diet}}$ (11.1‰) following Podelsak et al., 2008, B) Large mammal $\epsilon^*_{\text{enamel-diet}}$ (14.1‰) following Cerling and Harris (1999).

